doi:10.1016/j.jmb.2007.04.021 J. Mol. Biol. (2007) 369, 1333–1352

JMB

Available online at www.sciencedirect.com

ScienceDirect

ELSEVIER

Distinctive Topologies of Partner-switching Signaling Networks Correlate with their Physiological Roles

Oleg A. Igoshin[1], Margaret S. Brody[2], Chester W. Price[2] and Michael A. Savageau[1]*

[1]*Department of Biomedical Engineering, University of California, Davis, CA 95616 USA*

[2]*Department of Food Science University of California, Davis CA 95616, USA*

**Corresponding author*

Regulatory networks controlling bacterial gene expression often evolve from common origins and share homologous proteins and similar network motifs. However, when functioning in different physiological contexts, these motifs may be re-arranged with different topologies that significantly affect network performance. Here we analyze two related signaling networks in the bacterium *Bacillus subtilis* in order to assess the consequences of their different topologies, with the aim of formulating design principles applicable to other systems. These two networks control the activities of the general stress response factor σ^B and the first sporulation-specific factor σ^F. Both networks have at their core a "partner-switching" mechanism, in which an anti-sigma factor forms alternate complexes either with the sigma factor, holding it inactive, or with an anti-anti-sigma factor, thereby freeing sigma. However, clear differences in network structure are apparent: the anti-sigma factor for σ^F forms a long-lived, "dead-end" complex with its anti-anti-sigma factor and ADP, whereas the genes encoding σ^B and its network partners lie in a σ^B-controlled operon, resulting in positive and negative feedback loops. We constructed mathematical models of both networks and examined which features were critical for the performance of each design. The σ^F model predicts that the self-enhancing formation of the dead-end complex transforms the network into a largely irreversible hysteretic switch; the simulations reported here also demonstrate that hysteresis and slow turn off kinetics are the only two system properties associated with this complex formation. By contrast, the σ^B model predicts that the positive and negative feedback loops produce graded, reversible behavior with high regulatory capacity and fast response time. Our models demonstrate how alterations in network design result in different system properties that correlate with regulatory demands. These design principles agree with the known or suspected roles of similar networks in diverse bacteria.

Keywords: sigma factor; sporulation; design; stress; feedback

Introduction

The ability of cells to respond to environmental stimuli with differential gene expression is key to the diversity of life. One approach to understand the dynamic and functional properties of such responses involves studying the organization of the signaling networks that control them. Even though the underlying diversity of these networks is enormous, some common motifs are repeated in different contexts.[1–5] In many cases this appears to reflect divergent evolution from a common origin, since these network motifs comprise modules assembled from homologous proteins.

Upon close examination, differences become evident even in apparently similar networks that function in different physiological contexts. These differences can be divided into parametric or structural categories. Parametric differences have to do with variability of biochemical parameters whereas structural differences have to do with

Present address: O. A. Igoshin, Department of Bioengineering, MS-142, Rice University, Houston, TX 77251-1892, USA.

E-mail address of the corresponding author: masavageau@ucdavis.edu

variations in network organization, such as additional reactants, interactions or reactions. The structural variations are thought to reflect more significant evolutionary changes and therefore are more likely to correlate with specific physiological demands on the network. To reveal such correlations and the underlying design principles of the biochemical circuitry, we have used the method of mathematically controlled comparison.[6–9] This method facilitates the analysis of network performance by concentrating on structural differences; it introduces mathematical constraints to ensure that the observed differences in systemic behavior of alternative designs are a result of differences in network topology rather than accidental differences in the values of the kinetic parameters. Here we examine the key features in the designs for the partner-switching networks that regulate activity of the σ^B and σ^F sigma factors in the bacterium *Bacillus subtilis*. This partner switching mechanism is widely distributed among eubacteria and can be configured to accomplish different signaling tasks.[10–15] In *B. subtilis* it regulates two sigma factors, σ^B and σ^F, each of which controls a distinctive stress response.

σ^B controls a general stress regulon encoding more than 150 products that protect against diverse future challenges.[11,16] This general stress response is triggered by a broad array of energy and environmental stimuli, and loss of σ^B function leads to increased sensitivity to acid, cold, heat, ethanol, osmotic and oxidative stress.[17] The response is readily reversible, providing the cell with a flexible, moderate answer to growth-limiting stresses. By contrast, σ^F is one of five specialized sigma factors that control the sporulation process, an essentially irreversible program marked by an asymmetric division that produces two cell types, a mother cell and a smaller forespore, each with a different developmental fate.[18,19] The sporulation process is induced by a combination of nutritional, cell density, and DNA replication signals, and it results in the production of a metabolically inert endospore that is highly resistant to damage by heat, desiccation, solvents, and UV light. Significantly, σ^F is key to this process, and its specific activation in the forespore compartment initiates a chain of events that leads to activation of subsequent sigma factors in both the mother cell and forespore.[18,19]

The activities of σ^F and σ^B are controlled by similar signaling networks that function *via* the partner-switching mechanism[11,18–20]. The essential feature of this mechanism is the control of protein–protein interactions by means of serine or threonine phosphorylation. The implementation of this mechanism in the σ^F and σ^B networks is shown in Figure 1(a) and (b). Free sigma factor is capable of associating with RNA-polymerase core (not depicted in Figure 1) and activating transcription of the sigma-specific regulon. Prior to receiving the activation signal, an anti-sigma factor (either SpoIIAB or RsbW; henceforth abbreviated AB or W) binds to its respective sigma factor and prevents its association with RNA polymerase, turning the system OFF. Under these conditions, the anti-sigma factor also acts as a serine kinase that phosphorylates its cognate anti-anti-sigma factor (either SpoIIAA or RsbV; AA or V); the phosphorylated form of the anti-anti-sigma factor has low affinity for the anti-sigma factor and they quickly dissociate. This kinase activity of the anti-sigma factor (either AB or W) requires the presence of ATP in its catalytic site; during phosphorylation ATP is hydrolyzed to ADP, which must be exchanged for another ATP before the next round of phosphorylation. In the cartoon models shown in Figure 1, specificity in signal reception is largely provided by an input phosphatase and is governed by the association of a particular N-terminal sensing domain with a C-terminal PP2C domain.[11,18,19] This specific phosphatase (either SpoIIE or RsbP/U) activates the anti-anti-sigma factor by dephosphorylating it, thereby turning the system ON. The unphosphorylated anti-anti-sigma factor attacks the anti-sigma/sigma factor complex to induce sigma factor release. Thus, in both networks the level of sigma factor capable of binding to RNA polymerase is determined by the interplay between phosphorylation and dephosphorylation of the anti-anti-sigma factor.

Although the networks controlling σ^F and σ^B share the core of the partner switching mechanism, genetic, biochemical and biophysical studies have identified several important differences that are not conveyed by the simple models shown in Figure 1(a) and (b). Some of these differences are parametric. For example, the equilibrium dissociation constants of ATP and ADP with the anti-sigma factor are in the micromolar range for AB, whereas they are in the millimolar range for W.[21–24] This is thought to render the kinase activity of W sensitive to the ATP concentration within the cell, thereby providing an additional mechanism for sensing energy stress that complements the RsbP energy phosphatase. In addition to these parametric differences, significant structural differences exist between the networks, and these structural differences are our focus here: (1) Presence of a long-lived complex in the σ^F network (see Figure 1(c)). After phosphorylation and release of the AA anti-anti-sigma factor, the AB anti-sigma factor has ADP in its catalytic site. Binding another molecule of AA then locks AB-ADP in a long-lived complex incapable of exchanging ADP for ATP, and therefore incapable of phosphorylating AA to free itself.[21,25–28] Under these conditions, AA must dissociate in order to allow AB to exchange ATP for ADP, which permits the reaction cycle to resume. In our previous paper[29] we referred to this long-lived complex as a "dead-end" complex. Such a dead-end complex was originally identified by biochemical analysis of AA-AB, and was not found by similar analysis of the corresponding V-W regulators in the σ^B network.[21,22,24,25,28,30] These results argue that the complex of V, W and ADP is capable of rapid exchange of ATP for ADP without requiring the prior dissociation of V, and, therefore, is neither long-lived nor dead-end.

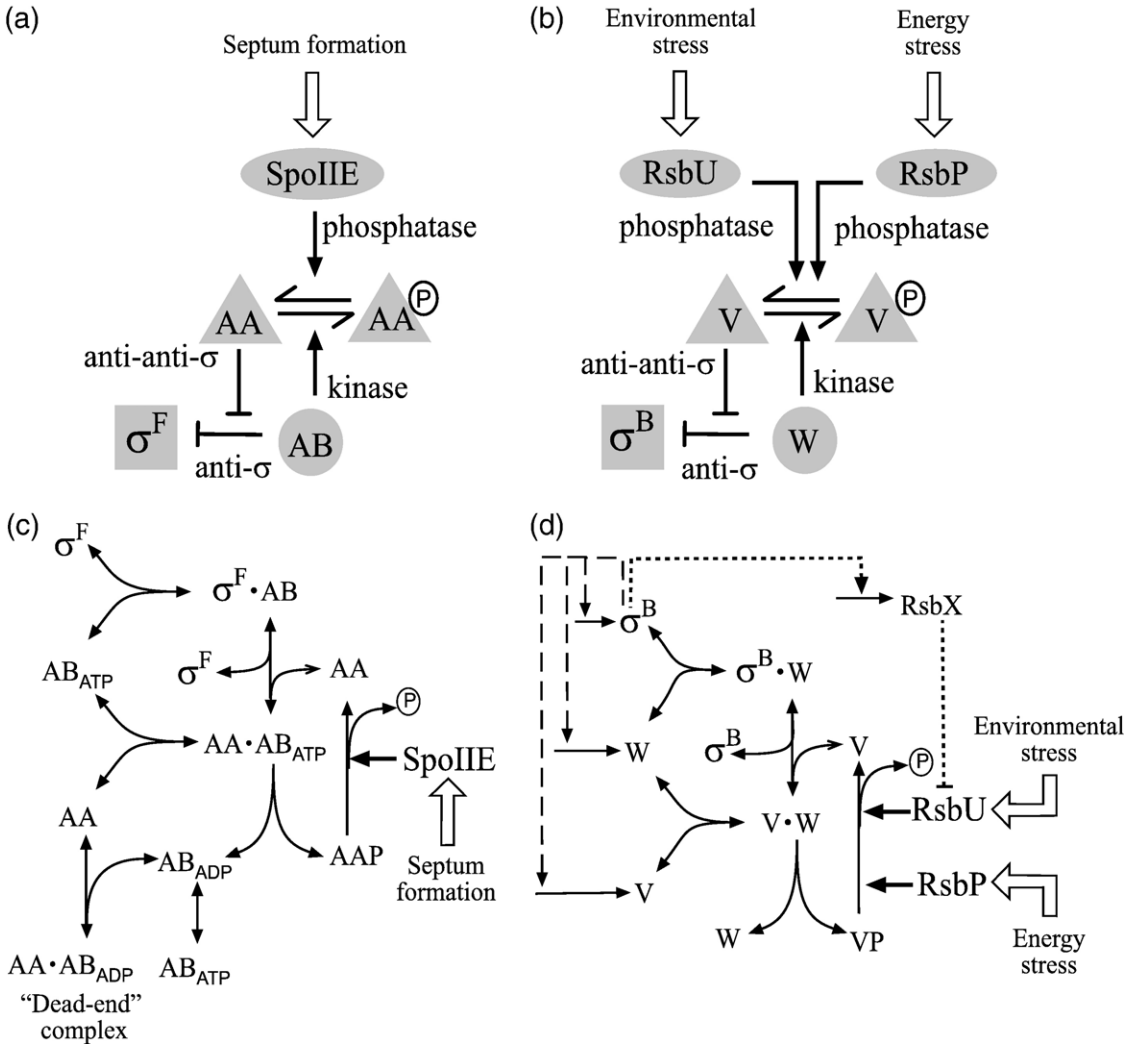

Figure 1. Conceptual ((a) and (b)) and kinetic ((c) and (d)) models of the partner-switching networks regulating σ^F and σ^B. For simplicity, only one subunit of the anti-sigma factor dimer is shown, and binding of sigma to RNA polymerase core is omitted as it does not affect the partner-switching equilibrium (see Modeling Procedures). (a) Level of free σ^F is determined by the level of unphosphorylated SpoIIAA anti-anti-sigma (AA), where P indicates serine phosphate (see the text). Activity of the SpoIIE phosphatase in the forespore increases upon formation of the asymmetric sporulation septum, turning the system ON. (b) Level of free σ^B is determined by the level of unphosphorylated RsbV anti-anti-sigma (V). Activity of either the RsbU environmental phosphatase or the RsbP energy phosphatase increases when a stress is perceived, turning the system ON. (c) Formation of a long-lived, dead-end complex in the σ^F network. The SpoIIAB anti-sigma factor (AB) with ATP in its catalytic site can phosphorylate and release the AA anti-anti-sigma factor, leaving AB associated with ADP in a non-catalytic complex. The binding of another AA molecule locks AB in this state. (d) Feedback loops in the σ^B network. Genes encoding σ^B, its anti-sigma RsbW (W) and anti-anti-sigma V lie in the σ^B-controlled *sigB* operon. The resulting feedback loops are shown by broken lines. An additional feedback loop through the RsbX phosphatase, which acts indirectly *via* the environmental-stress branch of the network, is shown by the dotted line. Each of the nodes containing W and its complexes are assumed to be in equilibrium, with a mixed population of ATP, ADP and nucleotide-free forms, so no explicit nucleotide exchange is shown.

(2) Feedback loops regulate the synthesis of core components of the σ^B network (see Figure 1(d), broken lines). Genes encoding σ^B and its partner-switching regulators V and W lie within a σ^B-controlled operon,[31] thereby manifesting both positive and negative feedback loops that would operate under either energy or environmental stress. In contrast, the *spoIIA* operon encoding AA, AB and σ^F is transcribed in predivisional cells by a non-cognate sigma factor, σ^H.[19] Therefore, no such feedback loops exist at the time of asymmetric septum formation, when σ^F is initially activated in the forespore compartment. A later round of read-through transcription from the upstream *dacF* gene does extend into the *spoIIA* operon, and this later round is under σ^F (and subsequently σ^G) control.[32–36] However, *dacF* transcription does not commence until 2.5 h after the asymmetric septum is formed. Thus this potential autocatalytic feedback loop is not relevant for the commitment-to-sporulation switch that we are considering here.

(3) An additional negative feedback loop is present exclusively in the environmental-stress branch of the

σ^B network (see Figure 1(d), dotted line). Here the activity of the environmental-stress phosphatase, RsbU, is indirectly down-regulated by the RsbX feedback phosphatase, a component of another partner-switching network (not shown) that modulates RsbU.[37–41] The gene encoding RsbX also lies within the σ^B-controlled operon that encodes σ^B and its network partners V and W.[31]

We and others have recently published mathematical models of the σ^F regulatory network.[29,42] The comparison of these two models is beyond the scope of this work and will be presented elsewhere. Nonetheless, while there are clear differences in the assumptions that underlie the two models, the essential conclusions of our work discussed here and by Igoshin *et al*.[29] are not significantly affected. Here we modify our previous σ^F model to describe the partner-switching mechanism of the σ^B network. To elucidate the impact of the three structural differences outlined above, we performed a series of mathematically controlled comparisons in which one or another key element of each model was altered and tested for its effect on network performance. The results of this analysis suggest that the differences in network organization correlate closely with their different physiological roles.

Results

By incorporating biochemical, biophysical and genetic data from the literature we constructed mathematical models of the σ^B and σ^F signaling networks. (For details of the modeling procedures and parameters assigned to the various reactions, please see Modeling Procedures.) Such modeling integrates all the relevant system components, imposes important thermodynamic constraints, and uses uniform criteria to characterize the steady state and dynamic performance of each network. Our goal was to elucidate the role and physiological consequence for each of the distinctive topological elements in the two networks. We therefore analyzed the performance of each network individually, using a series of mathematically controlled comparisons between a wild-type network and various hypothetical alternative designs in which one of the topological elements was altered.

Role of dead-end complex formation

An essential feature of the σ^F network is the formation of a long-lived, non-catalytic dead-end complex between the AB anti-sigma factor, its AA anti-anti-sigma factor, and ADP.[21,22,25–28] We have previously shown[29] that this dead-end complex causes the σ^F network to behave as an essentially irreversible hysteretic switch. This system property was associated with the self-enhancing formation of the dead-end complex: higher concentrations of dephosphorylated AA lead to higher concentrations of the non-catalytic complex at the expense of the active, phosphorylating complex, leading to even higher concentrations of dephosphorylated AA and of the dead-end complex (see Igoshin *et al*.[29] for a discussion). Here we ask whether the dead-end complex shapes other network properties independently from its contribution to hysteresis. To this end we analyze mathematical models that either include or exclude the formation of the complex (see Modeling Procedures for details).

For comparison purposes we repeat part of our earlier analysis[29] in Figure 2(a). In this Figure, broken and continuous lines show the steady-state concentration of free sigma factor in the wild-type network, expressed as a function of the rate of AA anti-anti-sigma dephosphorylation. This rate is a key determinant of σ^F activity in cells. That is, increased phosphatase activity (together with depletion of the AB anti-sigma in the forespore compartment) serves to convey the morphological signal of asymmetric septum formation to activate expression of σ^F-dependent genes.[19,20,43] In this simulation, the concentration of AA anti-anti-sigma factor was chosen to exceed that of the AB anti-sigma factor (considered as a monomer) by 50%, the excess necessary for hysteretic bistability.[29]

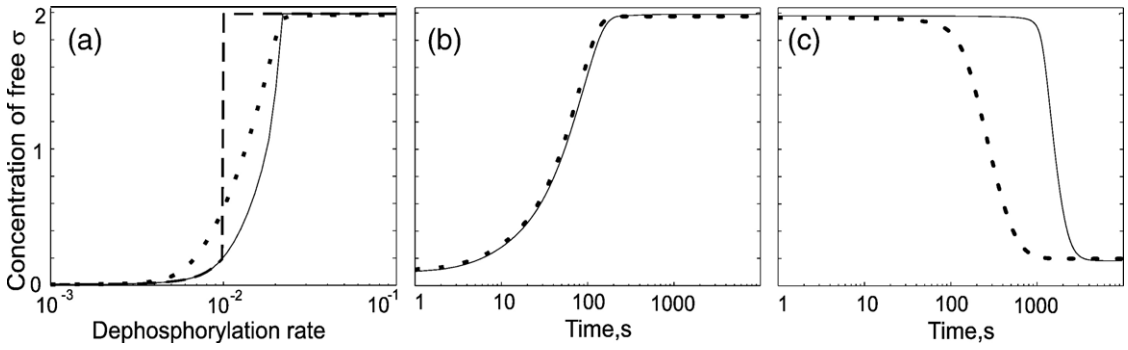

Figure 2. Comparison of σ^F networks with (broken or continuous lines) and without (dotted line) dead-end complex formation using parameter values that allow hysteresis ([AA]=1.5[AB]=9 μM; [σ^F]=2 μM) (a) Steady-state concentration of free sigma factor as a function of dephosphorylation rate. Under these conditions, when [AA] is in 50% excess to [AB], the network with the dead-end complex possesses two stable steady states, depending on system history. For comparison, only one steady state is possible for the network without the complex (see the text). (b) Dynamic response of free sigma factor to a step increase in rate of dephosphorylation. (c) Dynamic response of free sigma factor to a step decrease in the rate of dephosphorylation. Note that the time axes in kinetic plots (b) and (c) are represented with a logarithmic scale.

As we showed previously,[29] at intermediate dephosphorylation rates there are two stable, steady-state solutions for the concentrations of the network partners. The system can end up in either state depending upon the initial conditions. The continuous line in Figure 2(a) shows the steady-state solution corresponding to an initially OFF condition; this is the steady state for a low rate of dephosphorylation, with very little dead-end complex formed and most of the sigma factor in a complex with the AB anti-sigma factor. The broken line in Figure 2(a) shows the final steady-state solution corresponding to an initially ON condition; this is the steady state for a high rate of dephosphorylation, with most of the AA in the dead-end complex with the AB anti-sigma and most of the sigma factor free. The two stable steady states only exist for a range of dephosphorylation rates: at the boundaries of this range, the concentration of free sigma factor jumps from one branch of the solution to the other.

In our earlier modeling study this hysteretic behavior was shown to be associated with the self-enhancing formation of the dead-end complex coupled to the amount of dephosphorylated AA anti-anti-sigma factor.[29] To further test this argument mathematically and to see if dead-end complex formation has other effects on steady-state response, we compared the response of an otherwise similar network that only lacks the possibility of forming the complex. This alternative network was chosen to be as close to the reference system as possible, i.e. to produce the same concentration of free sigma factor at high and low rates of dephosphorylation (see Modeling Procedures for details). As shown by the dotted line in Figure 2(a), the network lacking the dead-end complex has a graded (continuous) response with only one stable steady state, corresponding to the rate of dephosphorylation. This strong effect of the dead-end complex on the steady-state properties of the system is in accord with the results of our earlier study.

In addition to these bistable steady-state properties, our earlier study[29] also predicted that the dynamic behavior of the system strongly contributes to the largely irreversible nature of σ^F activation: its partner-switching network is much faster to turn ON then to turn OFF. Here we ask whether this network property relates to the existence of the dead-end complex by comparing the transient responses of σ^F networks with and without this complex. Figure 2(b) shows the dynamic behavior of sigma factor activity (i.e. amount of free sigma factor) in response to a step increase in the rate of dephosphorylation for networks with (continuous line) and without (dotted line) formation of the dead-end complex. The time to turn ON sigma activity is about the same for both networks, with the network lacking the dead-end complex being slightly faster. By contrast, Figure 2(c) shows the dynamic behavior of sigma factor activity in response to a step decrease in the rate of dephosphorylation for networks with (continuous line) and without (dotted line) the dead-end complex. Significantly, the time to turn OFF sigma activity is much longer for the network containing the dead-end complex. For the network with the dead-end complex, the OFF time scale is determined by the lifetime of the complex, whereas for the network lacking the complex, the time scale is determined exclusively by the phosphorylation rate of the system. On the basis of the comparisons shown in Figure 2, we conclude that the presence of the dead-end complex has a marked effect on both the steady-state and dynamic properties of the σ^F signaling network.

Does this strong influence of the dead-end complex require conditions that promote hysteresis? Our model predicts that a 50% or greater excess concentration of AA anti-anti-sigma factor over AB anti-sigma factor is needed for hysteretic behavior to be observed. However, no reliable *in vivo* concentration measurements exist for these important parameters (see Igoshin *et al.*[29] for a discussion). Therefore, it was important to investigate the properties of the σ^F network using parameter values that do not lead to hysteretic bistability in order to determine if there might be other roles for the dead-end complex. For these simulations the concentration of AA anti-anti-sigma factor was chosen to be equal to that of the AB anti-sigma factor (considered as a monomer); under these conditions hysteresis is absent.[29] As expected from our previous study, with these parameter values the σ^F network displays a graded steady-state response lacking hysteresis (Figure 3(a), continuous line). The network without the possibility of forming the dead-end complex produces a very similar response (Figure 3(a), dotted line). Thus the steady-state effect of the dead-end complex is dependent on parameter values. However, formation of the dead-end complex still slows the transient response when turning OFF σ^F activity even in a network lacking hysteresis (Figure 3(b)). In response to an instant decrease of the dephosphorylation rate, the network lacking the dead-end complex (Figure 3(b), dotted line) turns OFF several-fold faster than the σ^F network with the dead-end complex (Figure 3(b), continuous line). These effects of the dead-end complex on the dynamic properties of the network are therefore at least partly independent from hysteresis.

Role of autocatalytic feedback involving σ^B

The genes encoding the stress-response factor σ^B and two of its network partners lie in a σ^B-controlled operon resulting in three feedback effects: (i) the activation of σ^B synthesis by the sigma factor itself is a positive feedback effect; (ii) the concomitant up-regulation of the W anti-sigma factor, which binds and inactivates σ^B, is a negative feedback effect; and (iii) the up-regulation of the V anti-anti-sigma factor releases σ^B from W, thereby creating another positive feedback effect. The overall sign of the feedback depends on the values of the parameters that characterize these three processes. Delumeau *et al.*[24] demonstrated that σ^B and its network partners

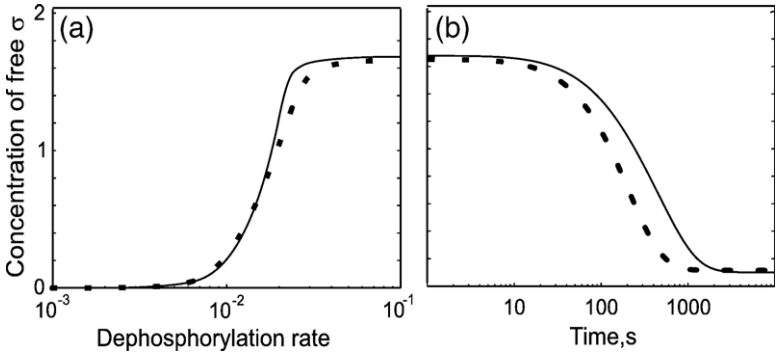

Figure 3. Comparison of σ^F networks with (continuous line) and without (dotted line) dead-end complex formation using values that preclude hysteresis ([AA]=[AB]=6 μM; [σ^F]=2 μM). (a) Steady-state concentration of free sigma factor as a function of dephosphorylation rate. Under these conditions when [AA] is equal to [AB], the network with the dead-end complex possesses only one stable steady state; the network without the complex performs similarly. (b) Dynamic response of free sigma factor to a step decrease in the rate of dephosphorylation (compare to Figure 2(c)).

are found in similar ratios both before and after stress, with a two to threefold excess of W and V monomers over σ^B. These ratios are required by the stoichiometry of the partner switching mechanism: W functions as a dimer that binds two molecules of V or one molecule of σ^B.[24] We incorporated this observation into our model (see Modeling Procedures). In Appendix A we also investigate the physiological consequences of a violation of this assumption, i.e. what will happen when one of the partner switching regulators is removed from σ^B control.

To elucidate how these feedback mechanisms influence the systemic properties of the σ^B network, we performed mathematically controlled comparisons of the reference model with an alternative model lacking feedback effects, i.e. a system in which the synthesis of σ^B and its network partners is controlled by another, hypothetical sigma factor and is therefore independent of σ^B activity (see Modeling Procedures for details). For simplicity we show only the analysis of the V-W-σ^B autocatalytic feedback loops under energy stress conditions, i.e. when the special environmental feedback *via* RsbX is absent. Similar conclusions are obtained regarding the effect of V-W-σ^B feedback under environmental stress conditions (data not shown).

The results for the reference system (Figure 4(a), continuous line) show the steady-state concentration of free sigma as a function of the V anti-anti-sigma dephosphorylation rate. For the alternative system lacking feedback, it apparently is not possible to match both the pre-stress and maximum-stress activities of sigma to those of the reference system. We therefore compared the reference system with two alternatives: one in which we match the pre-stress level of free sigma factor and the other in which we match the maximum-stress level. The results for the first alternative (Figure 4(a), dotted line) show that matching the pre-stress level of free sigma leads to a lower post-stress level, whereas the results for the second alternative (Figure 4(a), broken line) show that matching the maximum-stress level of free sigma leads to a higher pre-stress level. Thus, in the absence of feedback effects, the network exhibits a trade-off between high levels of free sigma in the maximum-stress condition and low levels in the pre-stress condition, and the capacity for regulation (the ratio between the maximum and the minimum levels of free sigma

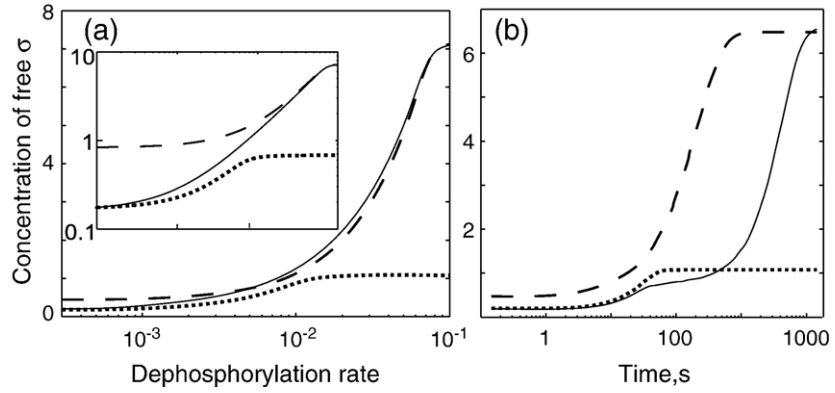

Figure 4. Comparison of σ^B networks with and without feedback resulting from σ^B-dependent transcription of the operon encoding σ^B and its network partners. These simulations were done under energy stress conditions to focus on the contribution of the V-W-σ^B feedback loop. (Figure 5 separately addresses the contribution of the RsbX feedback loop in the environmental signaling branch.) The continuous line corresponds to the reference (wild-type) system with feedback present. The broken line corresponds to an alternative system without feedback in which the rate of protein synthesis is set to match the level of free sigma at high dephosphorylation rates. The dotted line corresponds to an alternative system without feedback in which the rate of protein synthesis is set to match the level of free sigma at low dephosphorylation rates. (a) Steady-state concentration of free sigma as a function of the dephosphorylation rate. The inset shows the same curve plotted with log-log scales. (b) Dynamic response of free sigma following a step increase in the rate of dephosphorylation.

factor) is less than that of the reference system. Note that depending on the choice of the alternative system and the value of dephosphorylation rate, the level of free σ^B for the alternative systems can be either above or below the level of free σ^B for the reference system (Figure 4(a)). Thus, the overall influence of the feedback on the system output can be either positive or negative depending on the parameter values.

The intuitive reason for this trade-off is as follows. If no feedback is present, the total concentrations of sigma factor, anti-sigma factor and anti-anti-sigma factor proteins are fixed. Matching the maximum-stress level of sigma factor activity requires a high total concentration of network proteins, whereas matching the pre-stress level requires a low total concentration. Under pre-stress conditions, even when all of the V is phosphorylated, a certain concentration of σ^B is free from the W anti-sigma. According to our simulations, an increasing fraction of σ^B escapes from W with an increasing total concentration of proteins. Thus at the high total concentrations needed to achieve maximum-stress levels of activity, the pre-stress activity of σ^B is disproportionately high (Figure 4(a), broken line).

In addition to examining these steady-state effects, we also compared the dynamics of sigma factor release in the reference system with the same two alternative systems following a step increase in the rate of phosphorylation from the pre-stress level ($k_1^{max} = 10^{-3} s^{-1}$) to the maximum-stress level ($k_1^{max} = 70 \times 10^{-3} s^{-1}$). The results (Figure 4(b)) show that the alternative systems without feedback reach their steady state faster than the reference system with feedback. The dynamic response of the reference system occurs on two timescales. The initial response time is determined by the dephosphorylation rate, and the concentration of free sigma quickly reaches the total concentration of sigma factor in pre-stressed cells. In contrast, the second response time is determined by the rate of transcription/translation of σ^B operon products, and the concentration of free sigma eventually reaches the total concentration of sigma factor in maximum-stressed cells. The same trend is seen for the dynamics of sigma factor inactivation following a step decrease in the rate of dephosphorylation (results not shown). This is consistent with other studies showing that inducible catabolic systems with positive feedback are slower to respond than otherwise identical systems lacking such feedback.[6,44]

Thus, our comparisons indicate that the existence of the autocatalytic feedback loops with V, W and σ^B contribute to both the steady-state and dynamic properties of the network. The physiological consequences of these results are addressed in Discussion.

Role of negative feedback involving RsbX

The feedback mechanisms considered thus far operate on the σ^B network when activated by either energy or environmental stress. However, there is an additional feedback that operates exclusively in the environmental signaling branch of the network (Figure 1(d)). Here the activity of the RsbU phosphatase (which dephosphorylates the V anti-anti-sigma in response to environmental stress) is modulated by another partner-switching mechanism involving the RsbX feedback phosphatase.[37–41] The gene for RsbX also lies within the σ^B-controlled *sigB* operon, and increasing RsbX levels have a negative effect on RsbU activation. This has led to the proposal that RsbX serves to damp the environmental stress response and prevent continuous signaling during sustained stress.[38,39]

We investigated the role of this RsbX-dependent feedback mechanism by means of mathematically controlled comparisons. We compared the reference system that includes negative feedback *via* RsbX to an alternative system in which the RsbX concentration (or equivalently, the rate of its synthesis) is held constant independent of sigma factor concentration. The results were most dramatic when comparing the dynamics of σ^B activation following a step increase in the rate of V anti-anti-sigma dephosphorylation. Figure 5 shows the dynamic response of the reference system (continuous line) and that of two alternative systems. One alternative (broken line) corresponds to the case in which RsbX concentration is held constant at the pre-stress level of the reference system; the other (dotted line) corresponds to the case in which RsbX concentration is kept constant at the maximum-stress level of the reference system. For the latter alternative there is a good match to the reference in both the pre- and maximum-stress levels of free sigma factor, but the dynamics of moving from one stress condition to the other are very different. In the absence of RsbX-dependent negative feedback, the time dependence

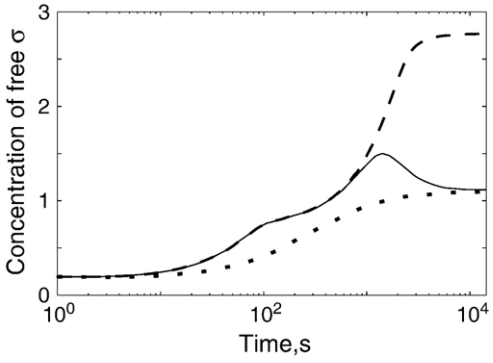

Figure 5. Comparison of σ^B networks with and without negative feedback involving RsbX. These simulations were done under environmental stress conditions. The dynamic behavior of the concentration of free sigma factor in the reference (wild-type) system with negative feedback (continuous line); in the alternative system without feedback and the RsbX concentration kept constant at the pre-stress level of the reference system (broken line); and in the alternative system without feedback and the RsbX concentration kept constant at the maximum-stress level of the reference system (dotted line).

of the increase in sigma factor concentration is monotonic. However, if the feedback is present as in the reference system, the concentration of sigma factor first overshoots the steady-state level found at maximum-stress, then gradually decreases to reach it. This time dependence results in a fast initial rate of sigma factor-dependent synthesis of stress proteins followed by a slower, steady-state synthesis (data not shown). We conclude that the RsbX negative feedback contributes to the ability of the network to mount a rapid response to a sudden environmental stress while retaining the ability to maintain the steady-state response appropriate for the continued presence of such a stress. This is consistent with other studies showing that repressible biosynthetic systems with negative feedback are faster to respond than otherwise identical systems lacking such feedback.[6,44]

Discussion

Essential modeling results are consistent with the physiological role of each network

Results of the mathematically controlled comparisons indicate how differences in σ^F and σ^B network organization result in qualitative differences in both the steady-state and dynamic behavior of each network. Additionally, inspection of the steady-state and dynamic properties of the reference (wild-type) systems in Figures 2–5 does allow direct comparison of the two networks, using common criteria. However, by itself such a direct comparison cannot reveal the fundamental basis of any difference in performance, and therefore it is not very illuminating. In contrast, the mathematically controlled comparisons of reference and alternative networks as performed here associate these differences in performance with differences in network topology. We find that these associated differences correlate well with the roles the networks play in the physiology of the organism.

Long-lived dead-end complex in the σ^F network

Our mathematical comparisons between σ^F networks with and without formation of the long-lived, non-catalytic AA-AB-ADP complex extend our previous analysis regarding the role of this complex in determining fundamental system properties: hysteresis and slow turn-OFF kinetics.[29] The simulations reported here demonstrate that these are the only two properties associated with dead-end complex formation. As a consequence of hysteresis, different threshold signals are required to turn ON or turn OFF expression of σ^F-dependent genes, as we described previously. Moreover, the simulations shown in Figure 2(c) indicate that even after reducing the dephosphorylation rate below the OFF threshold, the dynamics of turning off the system with the dead-end complex are much slower. In contrast, the network lacking the dead-end complex shows a graded response with faster OFF times. It should be noted that the slower turn-OFF of the σ^F network with the dead-end complex is observed even for parameter values that result in a graded steady-state response, i.e. hysteresis is absent (Figure 3(b)). Therefore, of the two network properties associated with dead-end complex formation, hysteresis is more dependent on parameter values than is slower turn-OFF.

As we argued previously,[29] these results make sense from a physiological point of view because the σ^F network controls a cell-fate decision. Once the asymmetric septum is formed, the decision to sporulate soon becomes irreversible[45] and the entire developmental program should be executed. Therefore, once σ^F activity is turned ON, it should be robustly protected from turning OFF due to fluctuations in kinetic parameters such as the rate of dephosphorylation. The slow temporal responsiveness of the system provides an additional level of protection by "filtering out" transient fluctuation in the values of kinetic parameters that might otherwise result in deactivation of σ^F. In contrast, σ^B activity is required to turn ON and OFF quickly in response to external conditions, and this readily reversible behavior correlates with the absence of a long-lived dead-end complex in the σ^B network.

Autocatalytic feedback in the σ^B network

The σ^B network possesses autocatalytic feedback loops resulting from σ^B-dependent control of the operon encoding V, W and σ^B. Our analysis shows that, depending on the choice of parameter values, the activity of σ^B for the system with autocatalytic feedback can be either above or below the activity for the system lacking this feedback. However, independent of these specific parameter values, the capacity for regulation (defined as the ratio between the maximum and the minimum levels of free sigma factor) is larger for the system with these feedback loops compared to the system lacking feedback. Therefore, we predict that autocatalytic feedback will reduce the trade-off that exists between a low, pre-stress level of σ^B activity and a high, maximum-stress level of activity (Figure 4(a)). Physiologically, the σ^B network must accommodate energy and environmental stresses that are highly diverse in both a qualitative and quantitative sense. The data of Akbar *et al.*[46] suggest that peak σ^B activity varies linearly with increasing ethanol stress. Presumably, higher levels of stress require higher σ^B activity, and indeed, under high-stress conditions σ^B-directed gene expression can account for 25% of total cellular protein synthesis.[47] On the other hand, inappropriate activation of σ^B, such as during exponential growth in unstressed cells, has a deleterious effect on growth and survival.[48] It is therefore important for the σ^B network to have a high capacity for regulation.

We argue that high capacity for regulation, while essential for the σ^B network, is irrelevant for the initial

function of σ^F network, which results in a digital ALL or NONE decision to activate σ^F in the forespore compartment and to keep it inactive in the mother cell. Additional physiological roles for σ^F later in forespore development may involve a subsequent increase of σ^F activity that autoregulation from the upstream *dacF* promoter could provide.[32–36] However, our simulations show that the initial role of σ^F in establishing differential gene expression between the two compartments and in making the commitment to sporulation does not need autocatalytic feedback. In accord with this hypothesis, mRNA transcribed from the σ^F-dependent *dacF* promoter does not appear until 2.5 h after septum formation,[32,34] well past the critical point at which the cell fate decision has been made.[19,45] Indeed, the role of this later, autoregulated transcription is presently unclear, because its interruption has no noticeable effect on sporulation.[34]

As a further link between feedback and the physiological role of the σ^B network, the temporal adaptation of the network containing this feedback has two stages, fast and slow (Figure 4(b)). Due to the presence of the slow stage, the response is not as rapid as for the alternative system lacking feedback. However, when the systems are matched so that they have the same level of pre-stress activity, the system with feedback is initially slower but actually achieves a significantly higher level of free sigma within a few minutes of stress exposure. Having such a two-stage response might allow the cell to generate sufficient σ^B activity on the fast timescale (to prevent deleterious consequences from a stress) while avoiding inappropriate generation of a full-scale stress response by transient signals.

The autoregulatory feedback in our σ^B model is implemented as a combination of two positive loops (up-regulation of σ^B and V expression) and one negative loop (up-regulation of W expression), with the network partners synthesized in nearly constant stoichiometric ratios. We argue that these loops are not completely independent from one another, and an appropriate balance among the players is necessary for the mechanism to work properly. To address this point, we investigated the consequences of removing individual feedback loops, as described in Appendix A. We conclude that presence of both positive feedback loops is essential for high regulatory capacity, i.e. if the expression of V is removed from σ^B control, regulatory capacity is significantly reduced. On the other hand, the existence of negative feedback *via* W is essential for the graded response of the σ^B network. If expression of W is removed from σ^B control, the network behaves as an ALL-or-NONE bistable switch, which, after activation, becomes insensitive to the rate of dephosphorylation. Thus all three components of the autoregulatory feedback are essential for its physiological role.

RsbX feedback in the σ^B network

The environmental branch of the σ^B signaling network contains an additional negative feedback mechanism involving RsbX. The system with this feedback manifests a non-monotonic dynamic release of σ^B (Figure 5). A physiological rationale for such a non-monotonic response appears to reflect two different demands on a stress-signaling network. When cells are first exposed to an environmental stress they must quickly synthesize the stress-response proteins that help them adapt to the new condition. However, when cells are subjected to prolonged environmental stress, they must continue to synthesize the stress-response proteins at a lower rate to replace those lost by damage and by dilution due to cell growth. It is clear that the network without the RsbX-dependent negative feedback could produce either (i) a rapid initial response coupled with too high a level of σ^B activity for prolonged stress (broken line in Figure 5), or (ii) a slower initial response coupled with an appropriate steady-state level of σ^B activity (dotted line). From this perspective, the systems with the RsbX-dependent negative feedback appear to have optimized both the rapid initial response and the appropriate prolonged response.

Therefore, the negative feedback mechanism involving RsbX is physiologically beneficial during a prolonged stress response controlled by the σ^B network. Why then does RsbX feedback operate only on the environmental branch of the network? We speculate that, in contrast to environmental stress, under energy stress it is more important to be efficient than fast, and overshooting is therefore not the best strategy.

Contrasting roles and mechanisms of feedback in the σ^B and σ^F networks

Positive feedback at the transcriptional level is often associated with bistable hysteretic behavior leading to the lock-ON of a developmental switch[49–52] Indeed, as part of the *B. subtilis* sporulation process, positive feedback tuned to morphological events serves to enhance transcription of the genes encoding σ^G and σ^K, the final two sigma factors controlling forespore and mother cell gene expression.[19] In contrast, the lock-ON of σ^F activity is achieved at the posttranslational level: the positive feedback is the result of the self-enhancing formation of the dead-end complex. Such a design guarantees an ALL or NONE steady-state response and fast dynamics to the turn-ON of σ^F activity on a biochemical time-scale. On the other hand, once turned ON, σ^F activity is protected from accidental turn-OFF by the long lifetime of the dead-end complex. While beneficial for the σ^F network, this design would be a disadvantage for the σ^B network. Activation of σ^B should be easily reversible and tunable to the magnitude of stress because excessive σ^B activity is deleterious for cell growth.[48] Apparently at odds with this requirement for reversibility, the positive feedback that results from autogenous regulation of the operon encoding V, W and σ^B would at first seem to parallel the classic bistable hysteretic switch, with its all or none behavior.[49–52] However, our simulations show that

despite this autoregulation, the σ^B network displays continuous (graded) response over a wide range of input signals and does not manifest bistability (Figure 4(a)). Such performance is in accord with the physiological demand and is ensured by a critical aspect of network design: positive feedback in the σ^B network is partially counteracted by a negative one, namely the parallel up-regulation of the synthesis of the W anti-sigma factor, which binds and inactivates σ^B. Indeed, elimination of this negative loop appears to convert the network into a bistable switch (Appendix A). What selective advantage might this elaborate feedback scheme confer? We have identified two physiologically beneficial effects of the autogenous regulation of *sigB*: increased capacity for regulation and a two-stage kinetic response. These effects apply equally to σ^B activation *via* the energy or environmental stress pathways. An additional negative feedback loop acting only in the environmental branch (*via* RsbX) gives rise to a non-monotonic dynamic response, which would elicit a burst-like synthesis of gene products needed to counteract the initial stress.

Autoregulatory feedback loops are conserved in homologous partner-switching networks that control a general stress response

Our modeling study suggests that the presence of autocatalytic feedback serves to increase the regulatory capacity of a partner-switching network. This increased capacity would be most useful in a network that must respond to diverse stresses of unpredictable magnitude, such as those that induce the general stress response. To ask whether this correlation between network architecture and physiological role could be extended to other Gram-positive bacteria, we compared the structures of operons encoding σ^B or σ^F orthologs. In each case, autocatalytic feedback was inferred to be present in those operons implicated in a general stress response. The results of our survey are presented in Tables 1 and 2 and discussed in Appendix B. The main conclusions are briefly summarized below.

Despite considerable variations of *sigB* operon structure among the low-GC Gram-positive bacteria, the striking feature of the general stress operons is the conservation of an apparently irreducible core: *rsbV* (encoding the V anti-anti-sigma), *rsbW* (W anti-sigma), and *sigB* (σ^B), all linked in an autocatalytic, σ^B-dependent transcription unit (Table 1). We therefore argue that unless there was selective pressure to maintain this network architecture, it would almost certainly be lost.[53,54] We conclude from this comparison of *B. subtilis* and its close relatives that networks associated with the general stress response must benefit from the presence of autocatalytic feedback.

Table 2. Autoregulation of two *sigB*-like factors in *S. coelicolor*

Gene	Function	Autoregulation	Reference
sigB	Osmotic, oxidative stress and differentiation	Yes	56
sigL	Sporulation	No	56
sigM	Sporulation	No	56
sigH-P1	Sporulation	No	82
sigH-P2	Salt-stress	Yes	82

Our prediction regarding a correlation between autocatalytic feedback and general stress is further extended by considering examples of partner-switching networks from *Streptomyces coelicolor*, a bacterium phylogenetically distant from *B. subtilis*. Even though differentiation and stress response networks in *S. coelicolor* are highly interrelated,[55,56] one may conclude that at least two sigma factors that participate not only in differentiation but also in a broader stress response are subject to complex autoregulation, with positive and negative feedback loops (Table 2 and Appendix B).

Can autoregulation of a partner-switching network be viewed as a signature of a general stress response function? The contrasting bacterial differentiation function controlled by partner switching primarily appears to be a cell fate decision that represents a digital ALL or NONE response. Thus, in this case there may be no physiological need for an increased regulatory capacity that would require autoregulation. As we have discussed, autoregulation does not impact the σ^F network at the time of asymmetric septum formation, when cell fate is decided. In the absence of experiment, it is not possible to rule out an immediate role for autoregulation in similar σ^F networks that operate in related bacteria. However, as a first approximation, the genes encoding the AA, AB and σ^F proteins in these bacteria all appear to be transcribed from a σ^H-like promoter directly upstream from the three-gene cluster, as they are in *B. subtilis* (see Appendix B).

Proposed experimental tests of σ^B model predictions

Our simulations are consistent with the published data on the *B. subtilis* σ^B network. However, no experiments have been done specifically to test the predicted roles of the feedback loops in shaping its *in*

Table 1. Autoregulation of *sigB* operons in other Gram-positive bacteria

Bacterium	SigB function	Operon structure	Autoregulation established
Bacillus licheniformis	General stress	p_A*RSTU* p_B?*VWBX*	By sequence analysis only [68]
Listeria monocytogenes	General stress	p_A*RSTU*p_B*VWBX*	83
Staphylococcus aureus	General stress	p_A*U*p_B*VWB*	84
Bacillus cereus	General stress	p_B*VWB*	73
Bacillus anthracis	General stress	p_B*VWB*	76

vivo performance. Our results indicate that elimination of the positive autocatalytic feedback *via* RsbV or σ^B (or elimination of the autocatalytic feedback loops altogether) will lead to a reduced regulatory capacity and an altered dynamic response. On the other hand, elimination of the negative feedback *via* RsbW is predicted to transform the network into a bistable ALL-or-NONE switch. In addition, our model predicts that loss of negative feedback *via* RsbX will eliminate the non-monotonic dynamic response of σ^B activity seen during prolonged exposure to environmental stress.

We suggest that these predictions can be tested using mutants corresponding to the hypothetical ones modeled here. To construct these mutants, one or another of the genes encoding the network partners could be removed from the *sigB* operon and placed elsewhere on the chromosome, under control of an inducible promoter to allow matching the removed regulator to its normal pre-or post-stress level. The responses of these mutants to energy or environmental stress could then be measured indirectly using well-characterized, σ^B-dependent *lacZ* fusions. These fusion results may not exactly replicate the simulations, which were based in part on an estimated rate of dilution and degradation of the V-W-σ^B partners. However, the relative differences in regulatory capacity and response should be clear. For the strain lacking the RsbW feedback it may be necessary to reconstitute the relevant part of the network in *E. coli* to avoid lethality of the ON bistable state. Such a reconstitution has been successfully accomplished for another purpose.[57]

Conclusions

Our aim was to use kinetic modeling to determine how topological variations affect network performance and correlate with physiological function. We constructed mathematical models and analyzed the partner-switching networks that control activity of two *B. subtilis* sigma factors: σ^F and σ^B. We demonstrated that despite clear conservation in the core mechanism of the networks, relatively small changes in network design significantly affect their transient and steady-state behavior. We suggest that these observed variations in performance correlate with the physiological role of each network. In the course of our modeling work we focused on qualitative differences in performance that are likely to hold over a wide range of parameter values. Therefore, we expect that the relationships between network design and physiological role that we describe here will hold for similar networks in other bacteria.

Modeling Procedures

We previously constructed a mathematical model for the partner-switching network that controls activation of σ^F.[29] Here we modify that model to describe the partner-switching mechanism of the σ^B network. To elucidate the impact of the structural differences between the two networks, we performed a series of mathematically controlled comparisons for each of these models, in which one or another critical topological element was altered.

It should be noted that the multiplicity of binding partners for the anti-sigma factor dimer complicates both models. For example, the σ^F model contains 27 species and 53 reactions, primarily due to the requirement to include the effects of slow nucleotide exchange from the dead-end complex. In contrast, the σ^B model can be reduced to ten species and up to 19 reactions if equilibrium in all nucleotide binding reactions is assumed. Despite this apparent complexity, many of the reactions can be characterized by the same kinetic parameters due to symmetry between the two dimer subunits and other simplifying assumptions. Nonetheless, an explicit presentation of the differential equations for both models would be overly cumbersome. We therefore chose to formulate a set of reactions and describe the corresponding kinetic mechanisms. This information can be transformed into differential equations using publicly available software.[58] SBML files with complete model descriptions are included in Supplementary Data, and the independent kinetic parameters that we used for both networks are summarized in Table 3.

Model reactions and notation

The reactions and notations used are summarized below (note that non-consecutive numbering of equations was chosen to keep the notation consistent with our previous paper[29]):

(1) Dephosphorylation of phosphorylated anti-anti-sigma factor:

$$AAP \rightarrow AA + P_i \tag{F.1}$$

(2) Reversible binding of anti-anti-sigma factor to anti-sigma factor with ATP in the catalytic site:

$$AB\text{-}AB_T + AA \leftrightarrow AB\text{-}AB_T \cdot AA \tag{F.2}$$

(3) Phosphorylation of the anti-anti-sigma factor and its subsequent dissociation:

$$AB\text{-}AB_T \cdot AA \rightarrow AB\text{-}AB_D + AAP \tag{F.3}$$

(4) Reversible binding of the anti-anti-sigma factor to an ADP bound form of the anti-sigma factor, producing a dead-end complex:

$$AB\text{-}AB_D + AA \leftrightarrow AB\text{-}AB_D \cdot AA \tag{F.4}$$

(5) Reversible nucleotide exchange in the catalytic site:

$$ATP + AB\text{-}AB_D \leftrightarrow AB\text{-}AB_T + ADP \tag{F.5}$$

In the reactions above *AB* stands for one of the four states (AB_T, AB_D, AB_TAA, AB_DAA) and only the state of the second subunit of the dimer is allowed to change.

(6) Binding of σ^F to an anti-sigma factor dimer subunit in either the AB_T or the AB_D state (denoted by AB_N):

$$AB_N\text{-}AB_N + \sigma \leftrightarrow AB_N\text{-}AB_N \cdot \sigma$$

$$AB_N\text{-}AB_N + \sigma \leftrightarrow AB_N \cdot \sigma\text{-}AB_N \tag{F.6}$$

(7) Reversible displacement of σ^F by anti-anti-sigma factor:

$$AB_N\text{-}AB_N \cdot \sigma + AA \leftrightarrow AB_N \cdot AA\text{-}AB_N + \sigma \tag{F.8}$$

Here we develop a framework that is also capable of describing the partner-switching network of σ^B and that allows comparison of both networks. Several important distinctions between the σ^F and σ^B networks are

Table 3. Parameter values used in our simulations

Parameter	Value, σ^B network	Value, σ^F network
k_2^a, k_{2a}^a	0.2 $\mu M^{-1}s^{-1}$	0.3 $\mu M^{-1}s^{-1}$
k_{2b}^a	0.5 $\mu M^{-1}s^{-1}$	
k_2^d, k_{2a}^d	5×10^{-3} s^{-1}	10^{-3} s^{-1}
k_{2b}^d	10^{-3} s^{-1}	
k_3	$5\times10^{-3}s^{-1}$	$9\times2\ 10^{-3}$ s^{-1}
k_4^a		0.3 $\mu M^{-1}s^{-1}$
k_4^d		10^{-3} s^{-1}
k_{5f}		1 s^{-1}
k_{5b}		0.2 s^{-1}
k_6^a	0.2 $\mu M^{-1}s^{-1}$	0.1 $\mu M^{-1}s^{-1}$
k_6^d	5×10^{-3} s^{-1}	10^{-3} s^{-1}
k_8^f	0.1 $\mu M^{-1}s^{-1}$	0.25 $\mu M^{-1}s^{-1}$
K	0.1 μM	0.1 μM
K_{inh}	0.5 μM	
k_9	7×10^{-4} s^{-1}	
$V_{10}^{max}, V_{11}^{max}$	4×10^{-3} μM/s	
V_{10}^{pr}, V_{11}^{pr}	1×10^{-5} μM/s	
K_s	2 μM	

summarized in the Introduction. These require modification of the reaction scheme to describe the σ^B network. First of all, in contrast to the σ^F network, the presence of ATP or ADP is not required for binding between anti-sigma factor W and its partners.[21,22,24,25] Moreover, nucleotide exchange is faster and does not require dissociation of the V anti-anti-sigma from W. Therefore, we chose not to explicitly treat the nucleotide-binding state of W, assuming that equilibrium between the nucleotide pools is rapidly reached and that the subscripts can be dropped. Delumeau *et al.*[24] presented evidence indicating a higher affinity for the binding of a second V to the V-W-W complex. Therefore, the binding of the first and second V are treated as separate reactions. In order to model feedback arising from σ^B controlling transcription of its own operon, protein synthesis and degradation are taken into account. The resulting reactions are presented below:

(1) Dephosphorylation of phosphorylated anti-anti-sigma factor:

$$VP \rightarrow V + P_i \tag{B.1}$$

(2) Reversible binding of the first anti-anti-sigma factor to anti-sigma factor dimer:

$$W\text{-}W + V \leftrightarrow W\text{-}W\cdot V \tag{B.2a}$$

(3) Reversible binding of the second anti-anti-sigma factor to the anti-sigma factor dimer:

$$W\text{-}W\cdot V + V \leftrightarrow W\cdot V\text{-}W\cdot V \tag{B.2b}$$

(4) Phosphorylation of the anti-anti-sigma factor and its subsequent dissociation:

$$W\text{-}W\cdot V \rightarrow W\text{-}W{+}VP$$

$$W\cdot V\text{-}W\cdot V \rightarrow W\cdot V\text{-}W{+}VP \tag{B.3}$$

(5) Binding of σ^B to an anti-sigma factor dimer:

$$W\text{-}W{+}\sigma \leftrightarrow W\text{-}W\cdot\sigma$$

$$W\text{-}W{+}\sigma \leftrightarrow W\cdot\sigma\text{-}W \tag{B.6}$$

(6) Reversible displacement of σ^F by anti-anti-sigma factor:

$$W\text{-}W\cdot\sigma + V \leftrightarrow W\cdot V\text{-}W{+}\sigma \tag{B.8}$$

(7) Protein degradation is assumed to be a first-order process combining "dilution" due to cell growth and specific or non-specific degradation by proteases.

$$Pr \rightarrow 0 \tag{B.9}$$

where Pr is any protein or protein complex in the σ^B network. Since little is known about the differences in the lifetimes of the proteins and protein complexes for the σ^B network, we assume them all to be the same.

(8) We assume that the synthesis rates for σ^B and its network partners are such that the proteins achieve concentrations near their stoichiometric ratios in the network:

$$aa \rightarrow \sigma + W{-}W + 2V \tag{B.10}$$

where *aa* stands for the amino acid pool, which is assumed to be constant. In the same fashion, we model synthesis of the RsbX protein (denoted X), which is involved in down-regulating the rate of VP dephosphorylation by RsbU, as:

$$aa \rightarrow X \tag{B.11}$$

We chose not to explicitly include the binding of sigma to core RNA polymerase in our models. The available evidence indicates that σ^F and σ^B bind their cognate anti-sigma factors with at least tenfold greater avidity than they bind to core.[24,30,59,60] Moreover, there is very little free core RNA polymerase in the cell, most of it occupied in transcribing DNA. Therefore, the core-binding reactions can be ignored.

Reaction kinetic mechanisms and kinetic parameters for the σ^B network

(1) The kinetics of association and dissociation of protein complexes, reactions (B.2a), (B.2b) and (B.6), are modeled as reversible mass action reactions. The corresponding rates of association and dissociations are denoted as k_i^a and k_i^d, respectively; here and below the subscript i stands for the equation number of the corresponding reaction. The equilibrium dissociation constant is denoted $K_i = k_i^d/k_i^a$. Delumeau *et al.*[24] used surface plasmon resonance (SPR) to obtain rate constants for association and dissociation of W (the anti-sigma factor of the σ^B system) and its network partners. The results are of the same order of magnitude as the corresponding parameters of the σ^F system: $k_{2a}^a \sim 0.9$ $\mu M^{-1}s^{-1}$, $k_6^a \sim 0.6$ $\mu M^{-1}s^{-1}$ and $k_{2a}^d \approx k_6^d \sim 6\times10^{-3}s^{-1}$. Note that the equilibrium dissociation constants obtained from these measurements are quite high, e.g. $k_6 \sim 100$ (nM). This indicates that around 25% of the sigma factor would be free if sigma and anti-sigma factor were mixed in a stoichiometric ratio with typical cellular concentrations of 1 μM. However, the results of independent experiments (Figure 2 of Delumeau *et al.*[24]) show that less than 10% of anti-sigma factor (and sigma factor) remains free under such conditions. This discrepancy may reflect the tendency of SPR to overestimate dissociation constants.[61,62] To account for this possibility we chose to decrease the measured rates of dissociation by tenfold. These reduced values are consistent with the data presented in Figure 2 of Delumeau *et al.*[24] Note that a similar reduction of dissociation rate was performed in our modeling of the σ^F network.[29] The results of Delumeau *et al.*[24] further indicate stronger binding of the second anti-anti-sigma factor to the anti-sigma factor dimer, i.e. binding cooperativity. In order to account for this effect we chose to further reduce the dissociation constant of the second anti-anti-sigma factor by a factor of 5.

(2) Delumeau *et al.*[24] measured the kinetics of anti-anti-sigma factor phosphorylation and found it to be linear in

time. The turnover rate was found to vary from $1.0\times10^{-3}s^{-1}$ to $1.0\times10^{-2}s^{-1}$, depending on ATP and ADP concentrations. Since this rate is much faster than the rate of complex formation, we use it to estimate the rate constant k_3.

(3) The dephosphorylation of the anti-anti-sigma factor is an enzymatic reaction performed by either of the two input phosphatases. Therefore, increase in phosphatase activity represents the signal for activating the transcription of σ^B-dependent genes. We model the rate of this dephosphorylation with a Michaelis-Menten-like expression:

$$k_1 = \frac{k_1^{\max}}{K + [VP]} \tag{1}$$

For the σ^B network, the activity of the RsbU environmental-signaling phosphatase is regulated by another partner-switch involving RsbX together with other proteins and protein complexes.[37–41] Since very little biochemical data are available for this second partner switch, we choose not to model it explicitly but rather phenomenologically by modifying equation (1). The influence of RsbX on the activity of the phosphatase will be treated empirically as non-competitive inhibition:

$$k_1 = \frac{k_1^{\max}}{(K + [VP])(1 + [X]/K_{\text{inh}})} \tag{2}$$

Here $[X]$ stands for the concentration of RsbX and K_{inh} is the effective inhibition constant, which is equal to the concentration of RsbX that results is a 50% reduction in phosphatase activity.

(4) Similar to our consideration of the σ^F network,[29] we can then treat the kinetics of the exchange reaction (B.8) as second-order mass action with rate constants k_8^f and k_8^b for the forward and backward reactions, respectively. As was the case in our σ^F model,[29] as long as no energy is consumed, the law of detailed balance provides a relationship among the equilibrium constants irrespective of the actual mechanism:

$$k_8^f/k_8^b = K_6/K_2 \tag{3}$$

(5) The degradation/dilution reaction (B.9) is described by first-order kinetics with rate constant k_9. We used data from β-galactosidase assays to estimate the decay rate for proteins. Experiments by Kim *et al.*[63] show a 50% decrease in β-galactosidase specific activity following a 15 to 30 min exposure to stress. This gives $k_9 \sim \log(2)/1000 \approx 7.0\times10^{-4}s^{-1}$.

(6) We approximate the complex multi-step process of protein synthesis by reactions (B.10) and (B.11) as first order processes in which the rate (flux) of synthesis depends on the concentration of free sigma factor as follows:

$$V_i = V_i^{\text{pr}} + V_i^{\max}[\sigma]/(K_S + [\sigma]) \tag{4}$$

Here V_i^{pr} is the rate of synthesis in the complete absence of σ^B activity; this reflects "priming" transcription from a σ^A-dependent promoter that regulates the upstream half of the σ^B operon and extends into the *rsbV-rsbW-sigB-rsbX* cluster.[64] $V_i^{\max}$ is the maximum rate of synthesis at saturating concentrations of sigma factor and K_S is the concentration of sigma factor at which half the maximum rate of synthesis is achieved. These parameters are estimated as follows. Delumeau *et al.*[24] showed that sigma factor concentration increased by 4 μM during the first 30 min of exposure to stress. This allowed us to estimate the rate of protein synthesis as $k_{10} \approx k_{11} \sim 2\times4$ μM/1800s ≈ 4.0×10^{-3} μMs^{-1}, where we assume that protein synthesis occurred at half its maximum rate in the experiments by Delumeau *et al.*[24] To estimate K_S we assumed it to be about one-half of the total concentration of RNA polymerase core in *B. subtilis* cells, $K_S \sim 2$ μM. (We used 5000 RNA polymerase molecules per cell as in *E. coli*, and a cell volume of 1.8×10^{-15} liter). This value is consistent with the results of Rollenhagen *et al.*[60] In contrast, there is no available data on the flux from the priming transcription V_i^{pr}. We choose the value 1.0×10^{-5} μMs^{-1} more than two orders of magnitude smaller than $V_i^{\max}$. The exact value of this priming flux does not affect the main conclusions of our analysis because under pre-stress conditions the major contribution to *sigB* (σ^B) expression comes from the second term in equation (4): even when all of the V is phosphorylated, a certain fraction of σ^B is free from the W anti-sigma. This free σ^B then sets the basal expression level for the *rsbV-rsbW-sigB-rsbX* cluster *via* the σ^B-dependent promoter preceding *rsbV*. This interpretation of the relative importance of priming *versus* autocatalytic transcription is consistent with the data presented in Figure 2 of Delumeau *et al.*[24] and in Figure 6 of Wise and Price.[64] This latter study showed that elimination of priming transcription did not impact activation of σ^B by energy stress. Although this value for priming transcription V_i^{pr} does not play a signifcant role in our reference system, it does affect the performance of the alternative networks considered in Appendix A.

The parameters used for numerical calculations are assembled in Table 3. For comparison we also included parameters for the σ^F network estimated by Igoshin *et al.*[29]

Mathematically controlled comparison of alternative designs

In order to reveal how variations in network design affect the physiological performance of signaling we used a technique known as mathematically controlled comparison.[6–9] This technique introduces mathematical constraints to ensure that the differences observed in the systemic behavior of alternative designs are a result of the specific differences in the network organization rather than of accidental differences in the values of the kinetic parameters.

In addition to differences in the values of the kinetic parameters, there are three major structural differences between the networks controlling σ^B and σ^F. As described in Introduction, these differences correspond to structural elements present in one network but absent in the other:

(i) In the σ^F network, formation of a long-lived, dead-end complex involving anti-sigma factor, its anti-anti-sigma factor, and ADP.

(ii) In the σ^B network, autocatalytic feedback involving σ^B regulation of the operon containing the genes for sigma factor, anti-sigma factor, and anti-anti-sigma factor.

(iii) In the σ^B network, a negative feedback involving σ^B regulation of the synthesis of RsbX protein, which indirectly inhibits dephosphorylation of the anti-anti-sigma factor during environmental stress.

To analyze the physiological consequence of these structural differences we performed three mathematical controlled comparisons. For each of the differences (i)–(iii) we chose the wild-type network as a reference system and compared it to an alternative design, a "mutant" network lacking this element. To ensure that any functional differences between the two can be attributed to differences in network organization and not to differences in

parameter values, we compared the systems under conditions of internal and external equivalence. Internal equivalence requires that the values of the corresponding parameters in the reference and alternative systems are the same. External equivalence requires that the systemic performances of the reference and alternative systems are made to match as closely as possible by suitably adjusting the values of the unique parameters, which represent degrees of freedom in the alternative system. After having introduced these constraints, we compared the two designs in terms of steady-state and transient responses. Specifically, we computed the steady-state concentration of free sigma factor as a function of the rate of anti-anti-sigma factor dephosphorylation k_1^{max} and the sigma factor dynamics following a sudden increase (or decrease) in k_1^{max}. Below we summarize comparisons (I)–(III) corresponding to differences (i)–(iii):

(I) We chose as the reference system the σ^F model that is characterized by reactions (F.1)–(F.8) and used the parameter values estimated from biochemical data.[29] As the alternative system we chose a system lacking formation of the long-lived complex, i.e. where anti-sigma factor has very little affinity for ADP, resulting in very rapid nucleotide exchange after phosphorylation. Formally, this system can be characterized by reactions (F.1), (F.2), (F.6), (F.8) and an effective phosphorylation reaction similar to (B.3):

$$AB\text{-}AB_T \cdot AA \rightarrow AB\text{-}AB_T + AAP \quad (5)$$

In this alternative system we essentially have only ATP bound in the catalytic site of AB. To emphasize the difference (i) we ignored protein synthesis and degradation. To ensure internal equivalence we assigned the same values for the corresponding kinetic parameters in the two systems, namely for those found in reactions (F.1), (F.2), (F.6), and (F.8). For external equivalence, first we required both systems to have the same (or similar) steady-state concentration of free sigma factor at very low and very high rates of anti-anti-sigma factor dephosphorylation k_1^{max}. These conditions were satisfied if we chose the total concentration of the corresponding proteins in the two networks to be the same. Second, we required both systems to make the transition between low and high-sigma levels at the same rate of anti-anti-sigma factor dephosphorylation: 50% of free σ^F in the alternative system is achieved at the geometric mean of the bistability region in the reference system. This second condition allowed us to determine the rate constant for the phosphorylation reaction (5) in the alternative system. For our simulations we had to decrease the catalytic rate of phosphorylation threefold to have the alternative network without the dead-end complex activate at the same dephosphorylation signal as the wild-type network with the complex.

(II) We chose as the reference system the σ^B model that is characterized by reactions (B.1)–(B.9) with the kinetics described by (1), (3) and (4). This model includes the feedback manifested by sigma factor-dependent transcription of the genes encoding sigma (σ^B), its anti-sigma (**W**), and its anti-anti-sigma (**V**). As the alternative system we chose the system lacking this feedback, which is characterized by reactions (B.1)–(B.10) with the kinetics described by (1) and (3) but with a constant rate of protein synthesis (i.e. independent of sigma factor concentration as opposed to equation (4)). For internal equivalence, we assigned the same values for the corresponding kinetic parameters in the two systems, namely for reactions (B.1)–(B.9). For external equivalence, we required both systems to have the same steady-state concentration of free sigma either in the low-stress condition (slow dephosphorylation of anti-anti-sigma) or in the high-stress condition (fast dephosphorylation of anti-anti-sigma). Either of these conditions was sufficient to fix the rate of protein synthesis V_{10} in the alternative system. Each of these alternative systems was compared to the reference system, as shown in Results.

(III) We chose as the reference system the full σ^B model that is characterized by reactions (B.1)–(B.11) with the protein synthesis rate given by equation (4) and with dephosphorylation rate given by equation (2). Under environmental stress, this model includes (i) specific feedback *via* RsbX-mediated inhibition of the RsbU environmental signaling phosphatase activity as well as (ii) general feedback *via* the sigma factor on the synthesis of sigma, anti-sigma, and anti-anti-sigma. As the alternative system we chose the system lacking feedback *via* RsbX, which is characterized by the reactions (B.1)–(B.10) but with a constant RsbX concentration. For internal equivalence, we assigned the same values for the corresponding kinetic parameters in the two systems, namely for those in reactions (B.1)–(B.10). For external equivalence, we required both systems to have the same steady-state concentration of free sigma either in the low-stress condition (slow dephosphorylation of anti-anti-sigma) or in the high-stress condition (fast dephosphorylation of anti-anti-sigma). Either of these conditions was sufficient to fix the concentration of RsbX in the alternative system. Each of these alternative systems was compared to the reference system, as shown in Results.

Software

Calculation of steady-state and dynamic responses was done using MATLAB© (MathWorks Inc, Natick, MA) and the Gepasi program.[65–67] SBML files for the models are available for download from Supplementary Data.

Acknowledgements

We thank Richard Losick for his helpful discussions and comments on the manuscript. This work was funded in part by grants from the US Public Health Service to M.A.S. (RO1-GM30054) and C.W.P. (RO1-GM42077).

Appendix A. Interplay of Autocatalytic Feedback Loops

In response to both energy and environmental stress, expression of the last four genes in the *sigB* operon (*rsbV-rsbW-sigB-rsbX*) is autogenously regulated by σ^B and (indirectly) by its co-transcribed network partners, V and W.[11] In Figure 4 we focused on the overall contribution of this feedback to the system properties of the network. Here we examine the individual contributions of the two positive loops (up-regulation of σ^B and V synthesis when σ^B is activated by stress) and the one negative loop (similar up-regulation of W synthesis). The available experimental data suggest that σ^B and its network partners are synthesized in similar stoichiometric

ratios before and during the stress response.[24] Here we investigate why such a design may have emerged in the course of natural selection. Simulations of the steady-state performance of the network were done in alternative networks, which are hypothetical mutants in which one of the three genes encoding the partner proteins (σ^B, V or W) was removed from σ^B control and placed in a separate, σ^B-independent transcription unit. Results were then calculated at different levels of constitutive expression for the removed gene. For clarity we performed the simulations under energy stress conditions, in which the RsbX negative feedback loop makes no contribution to the outcome.

As shown in Figure 4(a) of the main text, elimination of all three feedback loops significantly decreases capacity for regulation, i.e. introduces a trade-off between pre-stress and maximum-stress levels of sigma factor. The presence of both positive components of the feedback is required for the wide regulatory capacity characteristic of the wild-type network. If the expression of V is removed from σ^B control, the regulatory capacity of the system is significantly reduced (Figure A1(a)); the same effect is obtained if the expression of σ^B is removed (Figure A1(b)).

Notably, eliminating the negative component of the feedback by removing W expression from σ^B control leads to even more drastic changes in system performance. As shown in Figure A2, the σ^B network without W feedback behaves as an ALL-or-NONE bistable switch. The three panels (a)–(c) correspond to three different values of W synthesis flux, a parameter that significantly affects both the qualitative and quantitative behavior of the mutant network. This parameter would vary depending upon the strength of the promoter controlling the hypothetical σ^B-independent transcription unit containing the W gene. Figure A2(a) depicts the case for low flux, a level of W synthesis only slightly higher than that resulting from priming transcription in wild-type cells, i.e. in the complete absence of any basal σ^B activity (see Modeling Procedure for details). Figure A2(b) shows the case for intermediate flux, the level of W synthesis corresponding to the pre-stress level of W in wild-type cells. Here W concentration will be substantially higher than for Figure A2(a) but much lower than for Figure A2(c). Figure A2(c) shows the case of high flux, the level of W synthesis corresponding to the maximum-stress level of W in wild-type cells. Here the flux is comparable to that found in the wild-type system when the σ^B promoter is saturated.

The two stable steady states in each panel of Figure A2 are labeled ON and OFF. In the OFF state the concentration of free σ^B is so low that the genes encoding σ^B and V are expressed only at minimum levels by means of priming transcription. In the ON state the concentration of free σ^B is so high that the genes encoding σ^B and V are expressed at their maximum rate. The intuitive explanation of these results is as follows. For the simulations shown in Figure A2(a), W concentrations were chosen to be just slightly higher than that of σ^B and V when the latter are expressed *via* priming transcription. This ratio of W to σ^B is sufficient to keep sigma inactive at low V dephosphorylation rates. However, with increasing dephosphorylation rates, more σ^B is released from W and the σ^B-dependent promoter controlling σ^B and V gene expression becomes more active. This results in a multifold increase in the flux of σ^B and V synthesis. Thus, once the network moves to the ON state it becomes nearly insensitive to dephosphorylation rate because the concentration of the W anti-sigma is insufficient to control σ^B activity. The same explanation would hold for the ON state shown in Figure A2(b), with its intermediate levels of W. However, in contrast to Figure A2(a), the OFF steady state in Figure A2(b) is stable for all dephosphorylation rates as there would not be enough dephosphorylated V anti-anti-sigma present initially to counteract the higher level of W anti-sigma factor. So for the parameters chosen in Figure A2(b), variations of dephosphorylation rate will not affect the steady state of the system and it would remain in the initial condition, either ON or OFF. The simulations shown in Figure A2(c) are done with high W concentrations, corresponding to the level of W expression in stressed wild-type cells. As might be expected, the above arguments concerning the extreme stability of the OFF state in Figure A2(b) are still valid: this state is insensitive to changes in the dephosphorylation rate. On the other hand, the ON state now only exists for high dephosphorylation rates because the concentration of W in this simulation is comparable to the concentrations of σ^B and V when their genes are expressed from the fully activated σ^B-dependent promoter of the operon. Therefore, only when enough V is dephosphorylated to attack the W-σ^B complex will the ON state be achieved. Once the dephosphorylation rate decreases below a certain threshold, the system irreversibly jumps from the ON to the OFF state.

It should be noted that the bistability observed in the σ^B network, when the negative component of the autocatalytic feedback is eliminated, differs from the hysteretic bistability observed in the σ^F network because of the self-enforcing formation of the dead-end complex. In the latter case the network displays bistability only for an intermediate range of dephosphorylation rates and, therefore, σ^F activity can be turned ON and OFF with physiological levels of change in the dephosphorylation rate. Even though the turn OFF kinetics of the σ^F network are very slow, given enough time after a significant decrease in the dephosphorylation rate the network will go back to the OFF state. In contrast, the bistability observed in Figure A2 is not hysteretic as a function of the dephosphorylation rate, which is the physiological input signal for this system. ON (a), OFF (c), or both ON and OFF (b) steady states exist for all values of the dephosphorylation rate; transitions out of these states cannot be induced by changes in this rate, although such transitions might still be induced by changes

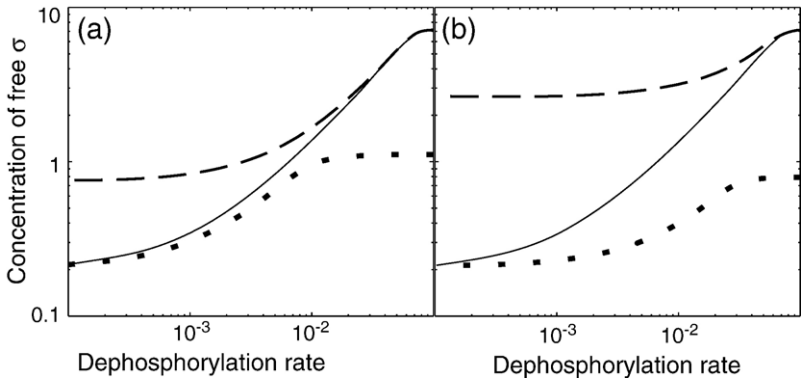

Figure A1. Removal of either positive autocatalytic loop affects steady-state performance of the σ^B network. (a) Elimination of σ^B control of V expression leads to reduced regulatory capacity. The reference (wild-type) steady-state response is shown by a continuous line. Broken and dotted lines correspond to maximum and pre-stress levels of V expression, respectively. (b) Elimination of σ^B control of σ^B expression also leads to reduced regulatory capacity. Line designations are as in (a), but here broken and dotted lines correspond to maximum and pre-stress levels of σ^B expression.

in other parameters or by stochastic fluctuations. In any case, such a design is not easily controllable and will not be physiologically meaningful for the stress response function.

The sum of these simulations shows that the correct balance of the V-W-σ^B autoregulatory feedback loops is crucial for the proper functioning of the σ^B network, with its high regulatory capacity and graded response.

Appendix B. Autoregulatory Feedback Loops in Homologous Partner-switching Networks

With the help of mathematical modeling we demonstrated that the presence of autocatalytic feedback loops serves to increase the regulatory capacity of a partner-switching network. We suggest that this increased capacity would be most useful in a network that responds to diverse inputs of various magnitudes, such as those that activate a general stress response. By contrast, increased regulatory capacity is not a requirement for the initial functioning of a partner-switching network that controls a cell fate decision. To ask whether this design principle could be extended to similar networks in other Gram-positive bacteria, we conducted a literature survey to correlate the presence of autocatalytic loops with the physiological roles of σ^B and σ^F factors and their network partners.

The results of this literature survey are presented in Tables 1 and 2 and in the discussion below. Notably, the structure of the *sigB* operon varies considerably among the low-GC Gram-positive bacteria, with different numbers of *rsb* (regulator of sigma-B) genes linked to the *sigB* structural gene (Table 1). These different linkage arrangements reflect the diversity of mechanisms that control the PP2C input phosphatases. For example, *Bacillus licheniformis*[68] and *Listeria monocytogenes*[69] possess

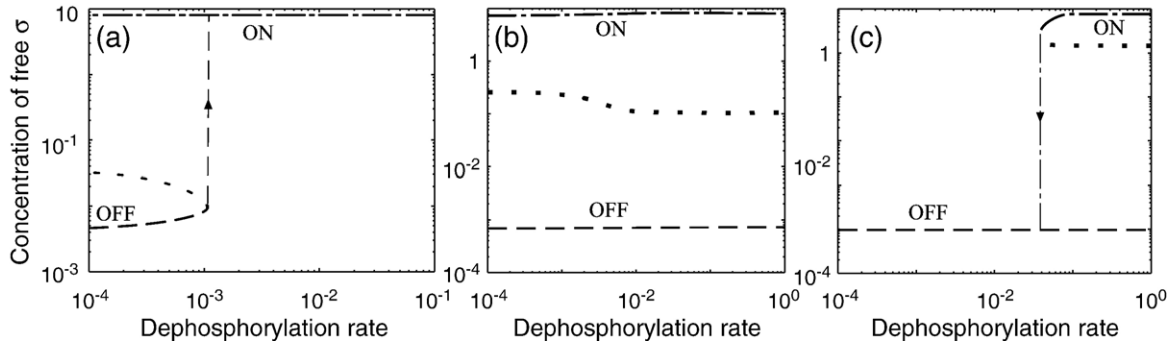

Figure A2. Elimination of σ^B control of W expression results in ALL or NONE bistability in the σ^B network. Stable steady-state solutions are shown by broken (OFF) and dash-dotted (ON) lines, whereas an unstable steady state between the two stable states is shown by the dotted line. The OFF state corresponds to a low level of σ^B, as would result from expression of its structural gene when the σ^B-dependent promoter of the *sigB* operon is not activated. The ON state corresponds to a high level of σ^B, as would result when the σ^B-dependent promoter of the *sigB* operon is fully activated by stress. (a) For low W expression (1.2×10^{-4} μMs^{-1}) the network displays two stable steady states only at low dephosphorylation rates; at high rates only the ON state exists. An irreversible transition from OFF to ON can be induced by an increasing dephosphorylation rate, as indicated by the up arrow. (b) For intermediate W expression (5×10^{-4} μMs^{-1}) the network displays two stable steady states over the entire range of dephosphorylation rates. (c) For high W expression (3×10^{-3} μMs^{-1}) the network displays two stable steady states only at high dephosphorylation rates; at low rates only the OFF state exists. An irreversible transition from ON to OFF can be induced by a decreasing dephosphorylation rate, as indicated by the down arrow. See the text for details.

the same operon structure as *B. subtilis* (Table 1). Based on the *B. subtilis* model, the *rsbRST* module in these organisms would encode a second partner switch that controls the RsbU environmental phosphatase, and the *rsbX* gene would encode a feedback phosphatase that damps continued signaling through this switch.[11] By contrast, in *Staphylococcus aureus* the RsbU phosphatase is controlled by a mechanism that remains to be determined, but that clearly differs from the *B. subtilis* model: the *rsbRST* module and the *rsbX* feedback phosphatase are missing from the *Staphylococcus* operon, and indeed from the entire genome.[70,71] Similar conclusions can be reached for the related *S. epidermidis sigB* operon.[70,72] In yet another variation, the gene for the input phosphatase of *B. cereus*, called *rsbY*, lies in a separate transcription unit downstream from the *sigB* operon.[73,74] RsbY phosphatase activity is thought to be controlled by a two-component system, with a CheY-like response-regulator domain covalently linked to the phosphatase domain. Consistent with this different input, the *B. cereus* genome encodes no *rsbRST* module, and no *rsbX* feedback phosphatase.[75] The related *B. anthracis sigB* operon has a similar structure.[76]

For the organisms listed in Table 1, σ^B activity is known to be induced by diverse stresses, which constitutes the hallmark of a general stress response. Consistent with this role, one striking feature of these operons is the conservation of an apparently irreducible core: the *rsbV* anti-anti-sigma gene, the *rsbW* anti-sigma gene, and *sigB*, all linked in an autocatalytic, σ^B-dependent transcription unit subject to the same feedback loops that we modeled here for the *B. subtilis* network. This conservation is maintained despite the variability of genes both upstream and down from the core. We therefore argue that unless there was selective pressure to maintain this network architecture, it would almost certainly be lost. We conclude from this comparison that for *B. subtilis* and its close relatives, partner-switching networks associated with a general stress response must benefit from the presence of immediate autocatalytic feedback.

By contrast, the two key features of the σ^F network are the presence of the dead-end complex and the absence of autocatalytic feedback at the time the cell fate decision is made. Neither of these features can be established without experiment. However, to a first approximation, we will take similar promoter and gene arrangement in related bacteria as presumptive evidence for a lack of autoregulation early on. The *B. subtilis spoIIA* operon (defined here as the *spoIIAA-spoIIAB-sigF* gene cluster) is initially transcribed from a σ^H-dependent promoter preceding *spoIIAA*[19] and subsequently from the σ^F/σ^G–dependent *dacF* promoter further upstream.[32–34] From the work by Park and Yudkin[77] and our own inspection of genomic sequences (not shown), it can be inferred that the *spoIIA* operons of representative Bacillus, Clostridium and Paenibacillus species are also under σ^H control (*B. coagulans*, *B. licheniformis*, *B. megaterium*, *B. sphaericus*, *B. stearothermophilus*, *C. acetobutylicum*, *C. tetani*, and *P. polymyxa*). Thus for *B. subtilis* and its close relatives, the networks associated with the control of the first compartment-specific sporulation factor (σ^F) apparently lack the immediate autocatalytic feedback loop found in the networks associated with the general stress factor (σ^B).

This correlation between immediate autocatalytic feedback and general stress is strengthened by considering partner-switching networks from *S. coelicolor*, a high-GC Gram-positive bacterium phylogenetically distant from the low-GC *B. subtilis*. The complex lifecycle of this bacterium is reflected in the extraordinary signaling and regulatory capability encoded in its large genome, including the structural genes for 66 sigma factors.[78,79] Among these, nine or ten are σ^B homologs, and four are particularly relevant to our discussion (Table 2). The σ^B, σ^L, and σ^M factors form an interesting regulatory cascade, with σ^B involved in both the general stress response and differentiation, whereas σ^L and σ^M seem to be primarily involved in differentiation.[56] Of these, only σ^B is clearly autoregulated, with the *rsbA* anti-sigma factor and *sigB* structural genes in one σ^B-dependent transcription unit and the *rsbV* anti-anti-sigma factor gene in another.[80] Thus the positive and negative autocatalytic feedback loops are maintained even with the separation of *rsbV* from its network partners. By contrast, *sigL* and *sigM* are apparently not autoregulated, but instead comprise part of a sigma cascade of $\sigma^B \rightarrow \sigma^L \rightarrow \sigma^M$.[56] The case of *S. coelicolor* σ^H is equally striking. The *sigH* gene is located in an operon together with the *ushX* gene encoding its anti-sigma factor.[81] This operon is expressed from at least two promoters: P1 is σ^H-independent and is active during differentiation, whereas P2 is σ^H-dependent and is active during osmotic stress.[82] Thus *sigH* expression appears to be regulated by both positive and negative feedback loops during stress response but not during differentiation. It is clear that the differentiation and stress response networks in *S. coelicolor* are highly interrelated,[55,56] and the mechanisms controlling sigma factor activity are not fully understood. However, one may conclude that sigma and anti-sigma pairs that participate not only in differentiation but also in a broader stress response are subject to autoregulation.

Supplementary Data

Supplementary data associated with this article can be found, in the online version, at doi:10.1016/j.jmb.2007.04.021

References

1. Wall, M. E., Hlavacek, W. S. & Savageau, M. A. (2004). Design of gene circuits: lessons from bacteria. *Nature Rev. Genet.* **5**, 34–42.
2. Lee, T. I., Rinaldi, N. J., Robert, F., Odom, D. T., Bar-Joseph, Z., Gerber, G. K. *et al.* (2002). Transcriptional regulatory networks in *Saccharomyces cerevisiae*. *Science*, **298**, 799–804.

3. Milo, R., Shen-Orr, S., Itzkovitz, S., Kashtan, N., Chklovskii, D. & Alon, U. (2002). Network motifs: simple building blocks of complex networks. *Science*, **298**, 824–827.
4. Conant, G. C. & Wagner, A. (2003). Convergent evolution of gene circuits. *Nature Genet.* **34**, 264–266.
5. Yeger-Lotem, E., Sattath, S., Kashtan, N., Itzkovitz, S., Milo, R., Pinter, R. Y. *et al.* (2004). Network motifs in integrated cellular networks of transcription-regulation and protein–protein interaction. *Proc. Natl Acad. Sci. USA*, **101**, 5934–5939.
6. Savageau, M. A. (1976). *Biochemical Systems Analysis : A Study of Function and Design in Molecular Biology.* Addison-Wesley Pub. Co, Reading, MA.
7. Voit, E. O. (1991). *Canonical Nonlinear Modeling: S-system Approach to Understanding Complexity.* Van Nostrand Reinhold, New York.
8. Alves, R. & Savageau, M. A. (2000). Extending the method of mathematically controlled comparison to include numerical comparisons. *Bioinformatics*, **16**, 786–798.
9. Alves, R. & Savageau, M. A. (2000). Comparing systemic properties of ensembles of biological networks by graphical and statistical methods. *Bioinformatics*, **16**, 527–533.
10. Koonin, E. V., Avarind, L. & Galperin, M. Y. (2000). A comparative-genomic view of the microbial stress response. In *Bacterial Stress Responses* (Storz, G. & Hengge-Aronis, R., eds), pp. 417–444, ASM Press, Washington DC.
11. Price, C. W. (2002). General stress response. In *Bacillus subtilis and its Closest Relatives: From Genes to Cells* (Sonenshein, A. L., Hoch, J. A. & Losick, R., eds), pp. 369–384, ASM Press, Washington, DC.
12. Beaucher, J., Rodrigue, S., Jacques, P. E., Smith, I., Brzezinski, R. & Gaudreau, L. (2002). Novel *Mycobacterium tuberculosis* anti-σ factor antagonists control σ^F activity by distinct mechanisms. *Mol. Microbiol.* **45**, 1527–1540.
13. Kozak, N. A., Mattoo, S., Foreman-Wykert, A. K., Whitelegge, J. P. & Miller, J. F. (2005). Interactions between partner switcher orthologs BtrW and BtrV regulate type III secretion in Bordetella. *J. Bacteriol.* **187**, 5665–5676.
14. Pané-Farré, J., Lewis, R. J. & Stülke, J. (2005). The RsbRST stress module in bacteria: a signalling system that may interact with different output modules. *J. Mol. Microbiol. Biotechnol.* **9**, 65–76.
15. Hua, L., Hefty, P. S., Lee, Y. J., Lee, Y. M., Stephens, R. S. & Price, C. W. (2006). Core of the partner switching signalling mechanism is conserved in the obligate intracellular pathogen *Chlamydia trachomatis*. *Mol. Microbiol.* **59**, 623–636.
16. Hecker, M. & Völker, U. (2001). General stress response of *Bacillus subtilis* and other bacteria. *Advan. Microb. Physiol.* **44**, 35–91.
17. Völker, U., Maul, B. & Hecker, M. (1999). Expression of the σ^B-dependent general stress regulon confers multiple stress resistance in *Bacillus subtilis*. *J. Bacteriol.* **181**, 3942–3948.
18. Piggot, P. J. & Losick, R. (2002). Sporulation genes and intercompartmental regulation. In *Bacillus subtilis and its Closest Relatives: From Genes to Cells* (Sonenshein, A. L., Hoch, J. A. & Losick, R., eds), pp. 483–518, ASM Press, Washington, DC.
19. Hilbert, D. W. & Piggot, P. J. (2004). Compartmentalization of gene expression during *Bacillus subtilis* spore formation. *Microbiol. Mol. Biol. Rev.* **68**, 234–262.
20. Yudkin, M. D. & Clarkson, J. (2005). Differential gene expression in genetically identical sister cells: the initiation of sporulation in *Bacillus subtilis*. *Mol. Microbiol.* **56**, 578–589.
21. Alper, S., Duncan, L. & Losick, R. (1994). An adenosine nucleotide switch controlling the activity of a cell-type-specific transcription factor in *Bacillus subtilis*. *Cell*, **77**, 195–205.
22. Alper, S., Dufour, A., Garsin, D. A., Duncan, L. & Losick, R. (1996). Role of adenosine nucleotides in the regulation of a stress-response transcription factor in *Bacillus subtilis*. *J. Mol. Biol.* **260**, 165–177.
23. Najafi, S. M. A., Harris, D. A. & Yudkin, M. D. (1997). Properties of the phosphorylation reaction catalyzed by SpoIIAB that help to regulate sporulation of *Bacillus subtilis*. *J. Bacteriol.* **179**, 5628–5631.
24. Delumeau, O., Lewis, R. J. & Yudkin, M. D. (2002). Protein-protein interactions that regulate the energy stress activation of σ^B in *Bacillus subtilis*. *J. Bacteriol.* **184**, 5583–5589.
25. Duncan, L., Alper, S. & Losick, R. (1996). SpoIIAA governs the release of the cell-type specific transcription factor σ^F from its anti-sigma factor SpoIIAB. *J. Mol. Biol.* **260**, 147–164.
26. Garsin, D. A., Duncan, L., Paskowitz, D. M. & Losick, R. (1998). The kinase activity of the antisigma factor SpoIIAB is required for activation as well as inhibition of transcription factor σ^F during sporulation in *Bacillus subtilis*. *J. Mol. Biol.* **284**, 569–578.
27. Lee, C. S., Lucet, I. & Yudkin, M. D. (2000). Fate of the SpoIIAB*-ADP liberated after SpoIIAB phosphorylates SpoIIAA of *Bacillus subtilis*. *J. Bacteriol.* **182**, 6250–6253.
28. Clarkson, J., Shu, J. C., Harris, D. A., Campbell, I. D. & Yudkin, M. D. (2004). Fluorescence and kinetic analysis of the SpoIIAB phosphorylation reaction, a key regulator of sporulation in *Bacillus subtilis*. *Biochemistry*, **43**, 3120–3128.
29. Igoshin, O. A., Price, C. W. & Savageau, M. A. (2006). Signalling network with a bistable hysteretic switch controls developmental activation of the σ^F transcription factor in *Bacillus subtilis*. *Mol. Microbiol.* **61**, 165–184.
30. Magnin, T., Lord, M. & Yudkin, M. D. (1997). Contribution of partner switching and SpoIIAA cycling to regulation of σ^F activity in sporulating *Bacillus subtilis*. *J. Bacteriol.* **179**, 3922–3927.
31. Kalman, S., Duncan, M. L., Thomas, S. M. & Price, C. W. (1990). Similar organization of the *sigB* and *spoIIA* operons encoding alternate sigma factors of *Bacillus subtilis* RNA polymerase. *J. Bacteriol.* **172**, 5575–5585.
32. de Lencastre, H. & Piggot, P. J. (1988). The *Bacillus subtilis spoIIA* locus is expressed at two times during sporulation. *FEMS Microbiol. Letters*, **51**, 109–112.
33. Schuch, R. & Piggot, P. J. (1994). The *dacF-spoIIA* operon of *Bacillus subtilis*, encoding σ^F is autoregulated. *J. Bacteriol.* **176**, 4104–4110.
34. Wu, J. J., Schuch, R. & Piggot, P. J. (1992). Characterization of a *Bacillus subtilis* sporulation operon that includes genes for an RNA polymerase σ factor and for a putative DD-carboxypeptidase. *J. Bacteriol.* **174**, 4885–4892.
35. Steil, L., Serrano, M., Henriques, A. O. & Völker, U. (2005). Genome-wide analysis of temporally regulated and compartment-specific gene expression in sporulating cells of *Bacillus subtilis*. *Microbiology*, **151**, 399–420.
36. Wang, S. T., Setlow, B., Conlon, E. M., Lyon, J. L., Imamura, D., Sato, T. *et al.* (2006). The forespore line of

gene expression in *Bacillus subtilis*. *J. Mol. Biol.* **358**, 16–37.
37. Kang, C. M., Brody, M. S., Akbar, S., Yang, X. & Price, C. W. (1996). Homologous pairs of regulatory proteins control activity of *Bacillus subtilis* transcription factor σ^B in response to environmental stress. *J. Bacteriol.* **178**, 3846–3853.
38. Yang, X., Kang, C. M., Brody, M. S. & Price, C. W. (1996). Opposing pairs of serine protein kinases and phosphatases transmit signals of environmental stress to activate a bacterial transcription factor. *Genes Dev.* **10**, 2265–2275.
39. Voelker, U., Luo, T., Smirnova, N. & Haldenwang, W. (1997). Stress activation of *Bacillus subtilis* σ^B can occur in the absence of the σ^B negative regulator RsbX. *J. Bacteriol.* **179**, 1980–1984.
40. Chen, C. C., Lewis, R. J., Harris, R., Yudkin, M. D. & Delumeau, O. (2003). A supramolecular complex in the environmental stress signalling pathway of *Bacillus subtilis*. *Mol. Microbiol.* **49**, 1657–1669.
41. Kim, T. J., Gaidenko, T. A. & Price, C. W. (2004). A multicomponent protein complex mediates environmental stress signaling in *Bacillus subtilis*. *J. Mol. Biol.* **341**, 135–150.
42. Iber, D., Clarkson, J., Yudkin, M. D. & Campbell, I. D. (2006). The mechanism of cell differentiation in *Bacillus subtilis*. *Nature*, **441**, 371–374.
43. Dworkin, J. & Losick, R. (2001). Differential gene expression governed by chromosomal spatial asymmetry. *Cell*, **107**, 339–346.
44. Hlavacek, W. S. & Savageau, M. A. (1996). Rules for coupled expression of regulator and effector genes in inducible circuits. *J. Mol. Biol.* **255**, 121–139.
45. Dworkin, J. & Losick, R. (2005). Developmental commitment in a bacterium. *Cell*, **121**, 401–409.
46. Akbar, S., Kang, C. M., Gaidenko, T. A. & Price, C. W. (1997). Modulator protein RsbR regulates environmental signalling in the general stress pathway of *Bacillus subtilis*. *Mol. Microbiol.* **24**, 567–578.
47. Bernhardt, J., Völker, U., Völker, A., Antelmann, H., Schmid, R., Mach, H. & Hecker, M. (1997). Specific and general stress proteins in *Bacillus subtilis*- a two-dimensional protein electrophoresis study. *Microbiology*, **143**, 999–1017.
48. Boylan, S. A., Rutherford, A., Thomas, S. M. & Price, C. W. (1992). Activation of *Bacillus subtilis* transcription factor σ^B by a regulatory pathway responsive to stationary-phase signals. *J. Bacteriol.* **174**, 3695–3706.
49. Monod, J. & Jacob, F. (1961). Teleonomic mechanisms in cellular metabolism, growth, and differentiation. *Cold Spring Harbor Symp. Quant. Biol.* **26**, 389–401.
50. Ferrell, J. E., Jr (2002). Self-perpetuating states in signal transduction: positive feedback, double-negative feedback and bistability. *Curr. Opin. Cell Biol.* **14**, 140–148.
51. Davidson, E. H., McClay, D. R. & Hood, L. (2003). Regulatory gene networks and the properties of the developmental process. *Proc. Natl Acad. Sci. USA*, **100**, 1475–1480.
52. Ptashne, M. (2004). *A Genetic Switch: Phage Lambda Revisited*, 3rd edit., Cold Spring Harbor Laboratory Press, Cold Spring Harbor, NY.
53. Lawrence, J. G. (2003). Gene organization: selection, selfishness, and serendipity. *Annu. Rev. Microbiol.* **57**, 419–440.
54. von Mering, C., Zdobnov, E. M., Tsoka, S., Ciccarelli, F. D., Pereira-Leal, J. B., Ouzounis, C. A. & Bork, P. (2003). Genome evolution reveals biochemical networks and functional modules. *Proc. Natl Acad. Sci. USA*, **100**, 15428–15433.
55. Viollier, P. H., Kelemen, G. H., Dale, G. E., Nguyen, K. T., Buttner, M. J. & Thompson, C. J. (2003). Specialized osmotic stress response systems involve multiple SigB-like sigma factors in *Streptomyces coelicolor*. *Mol. Microbiol.* **47**, 699–714.
56. Lee, E. J., Karoonuthaisiri, N., Kim, H. S., Park, J. H., Cha, C. J., Kao, C. M. & Roe, J. H. (2005). A master regulator σ^B governs osmotic and oxidative response as well as differentiation via a network of sigma factors in *Streptomyces coelicolor*. *Mol. Microbiol.* **57**, 1252–1264.
57. Scott, J. M., Smirnova, N. & Haldenwang, W. G. (1999). A Bacillus-specific factor is needed to trigger the stress-activated phosphatase/kinase cascade of σ^B induction. *Biochem. Biophys. Res. Commun.* **257**, 106–110.
58. Alves, R., Antunes, F. & Salvador, A. (2006). Tools for kinetic modeling of biochemical networks. *Nature Biotechnol.* **24**, 667–672.
59. Lord, M., Barilla, D. & Yudkin, M. D. (1999). Replacement of vegetative σ^A by sporulation-specific σ^F as a component of the RNA polymerase holoenzyme in sporulating *Bacillus subtilis*. *J. Bacteriol.* **181**, 2346–2350.
60. Rollenhagen, C., Antelmann, H., Kirstein, J., Delumeau, O., Hecker, M. & Yudkin, M. D. (2003). Binding of σ^A and σ^B to core RNA polymerase after environmental stress in *Bacillus subtilis*. *J. Bacteriol.* **185**, 35–40.
61. Schuck, P. & Minton, A. P. (1996). Kinetic analysis of biosensor data: elementary tests for self-consistency. *Trends Biochem. Sci.* **21**, 458–460.
62. Schuck, P. & Minton, A. P. (1996). Analysis of mass transport-limited binding kinetics in evanescent wave biosensors. *Anal. Biochem.* **240**, 262–272.
63. Kim, T. J., Gaidenko, T. A. & Price, C. W. (2004). In vivo phosphorylation of partner switching regulators correlates with stress transmission in the environmental signaling pathway of *Bacillus subtilis*. *J. Bacteriol.* **186**, 6124–6132.
64. Wise, A. A. & Price, C. W. (1995). Four additional genes in the *sigB* operon of *Bacillus subtilis* that control activity of the general stress factor σ^B in response to environmental signals. *J. Bacteriol.* **177**, 123–133.
65. Mendes, P. (1993). Gepasi- a software package for modeling the dynamics, steady-states and control of biochemical and other systems. *Comput. Appl. Biosci.* **9**, 563–571.
66. Mendes, P. (1997). Biochemistry by numbers: simulation of biochemical pathways with Gepasi 3. *Trends Biochem. Sci.* **22**, 361–363.
67. Mendes, P. & Kell, D. B. (1998). Non-linear optimization of biochemical pathways: applications to metabolic engineering and parameter estimation. *Bioinformatics*, **14**, 869–883.
68. Brody, M. S. & Price, C. W. (1998). *Bacillus licheniformis sigB* operon encoding the general stress transcription factor σ^B. *Gene*, **212**, 111–118.
69. Glaser, P., Frangeul, L., Buchrieser, C., Rusniok, C., Amend, A., Baquero, F. *et al.* (2001). Comparative genomics of Listeria species. *Science*, **294**, 849–852.
70. Gill, S. R., Fouts, D. E., Archer, G. L., Mongodin, E. F., Deboy, R. T., Ravel, J. *et al.* (2005). Insights on evolution of virulence and resistance from the complete genome analysis of an early methicillin-resistant *Staphylococcus aureus* strain and a biofilm-producing methicillin-resistant *Staphylococcus epidermidis* strain. *J. Bacteriol.* **187**, 2426–2438.
71. Wu, S., de Lencastre, H. & Tomasz, A. (1996). Sigma-B, a putative operon encoding alternate sigma factor of *Staphylococcus aureus* RNA polymerase: molecular

cloning and DNA sequencing. *J. Bacteriol.* **178**, 6036–6042.
72. Knobloch, J. K., Bartscht, K., Sabottke, A., Rohde, H., Feucht, H. H. & Mack, D. (2001). Biofilm formation by *Staphylococcus epidermidis* depends on functional RsbU, an activator of the *sigB* operon: differential activation mechanisms due to ethanol and salt stress. *J. Bacteriol.* **183**, 2624–2633.
73. van Schaik, W., Tempelaars, M. H., Wouters, J. A., de Vos, W. M. & Abee, T. (2004). The alternative sigma factor σ^B of *Bacillus cereus*: response to stress and role in heat adaptation. *J. Bacteriol.* **186**, 316–325.
74. van Schaik, W., Tempelaars, M. H., Zwietering, M. H., de Vos, W. M. & Abee, T. (2005). Analysis of the role of RsbV, RsbW, and RsbY in regulating σ^B activity in *Bacillus cereus*. *J. Bacteriol.* **187**, 5846–5851.
75. Anderson, I., Sorokin, A., Kapatral, V., Reznik, G., Bhattacharya, A., Mikhailova, N. *et al.* (2005). Comparative genome analysis of *Bacillus cereus* group genomes with *Bacillus subtilis*. *FEMS Microbiol. Letters*, **250**, 175–184.
76. Fouet, A., Namy, O. & Lambert, G. (2000). Characterization of the operon encoding the alternative σ^B factor from *Bacillus anthracis* and its role in virulence. *J. Bacteriol.* **182**, 5036–5045.
77. Park, S. G. & Yudkin, M. D. (1997). Sequencing and phylogenetic analysis of the *spoIIA* operon from diverse Bacillus and Paenibacillus species. *Gene*, **194**, 25–33.
78. Bentley, S. D., Chater, K. F., Cerdeno-Tarraga, A. M., Challis, G. L., Thomson, N. R., James, K. D. *et al.* (2002). Complete genome sequence of the model actinomycete *Streptomyces coelicolor* A3(2). *Nature*, **417**, 141–147.
79. Hahn, M. Y., Bae, J. B., Park, J. H. & Roe, J. H. (2003). Isolation and characterization of *Streptomyces coelicolor* RNA polymerase, its sigma, and antisigma factors. *Methods Enzymol.* **370**, 73–82.
80. Lee, E. J., Cho, Y. H., Kim, H. S., Ahn, B. E. & Roe, J. H. (2004). Regulation of σ^B by an anti- and an anti-anti-sigma factor in *Streptomyces coelicolor* in response to osmotic stress. *J. Bacteriol.* **186**, 8490–8498.
81. Sevcikova, B. & Kormanec, J. (2002). Activity of the *Streptomyces coelicolor* stress-response sigma factor σ^H is regulated by an anti-sigma factor. *FEMS Microbiol. Letters*, **209**, 229–235.
82. Sevcikova, B., Benada, O., Kofronova, O. & Kormanec, J. (2001). Stress-response sigma factor σ^H is essential for morphological differentiation of *Streptomyces coelicolor* A3(2). *Arch. Microbiol.* **177**, 98–106.
83. Becker, L. A., Cetin, M. S., Hutkins, R. W. & Benson, A. K. (1998). Identification of the gene encoding the alternative sigma factor σ^B from *Listeria monocytogenes* and its role in osmotolerance. *J. Bacteriol.* **180**, 4547–4554.
84. Senn, M. M., Giachino, P., Homerova, D., Steinhuber, A., Strassner, J., Kormanec, J. *et al.* (2005). Molecular analysis and organization of the σ^B operon in *Staphylococcus aureus*. *J. Bacteriol.* **187**, 8006–8019.

Edited by M. Gottesman

(Received 22 November 2006; received in revised form 9 April 2007; accepted 9 April 2007)
Available online 14 April 2007